Applied Water Science (2024) 14:189
https://doi.org/10.1007/s13201-024-02251-x

ORIGINAL ARTICLE

Development of desalination plants within the semi-enclosed Persian Gulf

Samad Rasoulpour[1] · **Hassan Akbari**[1]

Received: 22 April 2024 / Accepted: 28 July 2024 / Published online: 8 August 2024

Abstract

Although many desalination plants have been built in the countries around the Persian Gulf (PG) over the past decade, there exist crucial water demands in this region. Considering the limited water exchange between PG and the open seas, effluents more than the natural capacity of the PG will increase the sea-water salinity continuously. This excess salinity, in addition to threatening the marine ecosystems, endangers the water supply for many population centers. This study provides a comprehensive numerical analysis of the impact of existing and new desalination plants on the PG's salinity. In addition, the water residence time and pollutant extension have been investigated in the PG. There exist several concerns, especially in recent years about the probable threat of desalination growth in semi-enclosed seas such as PG. The effect of desalination plants on the mean salinity of PG is one the questions investigated in this research. Results demonstrate that the water residence times in the southern and northwestern regions are more than five years. This time is reduced to nearly 26 to 45 months in the eastern regions near the Strait of Hormuz. Generally, the desalination plants have a negligible effect on the salinity of PG in comparison with the climate conditions such as evaporation and water exchanges. Based on the results, a 50% increase in effluent discharge of existing desalination plants increases the average salinity of the PG by only 0.01 psu. However, the annual volume of net evaporation (that exits the clean water directly) is nearly 36 times more than the effluent discharge from the existing desalination plants. Furthermore, this value is almost 0.2% of the amount of water that enters the PG through the Strait of Hormuz. In spite of these findings, the regional effects can be significant in some parts of the PG. For example, the southern and western coasts of PG are generally more vulnerable to pollution than other areas. The main reason is the shallow water depth in these areas and the water recirculation pattern. Some sensitive local areas have been also addressed in this study. Among the studied regions, the coastlines at the northwest of PG and at the north the Qeshm Island are two susceptible areas. The findings of this study underscore the importance of considering a new integrated viewpoint in developing desalination plants within PG.

Keywords Desalination development · Hydrodynamic circulation · Numerical model · Salinity · Persian Gulf

Introduction

The Persian Gulf (PG) is a shallow, semi-enclosed sea. This gulf is connected to the Gulf of Oman through the Strait of Hormuz and extends from the mouth of the Arvand River to the Musandam Peninsula in Oman. With an area of 239,000 square kilometers and an average depth of 50 m, this gulf is the third largest gulf in the world. The average volume of water in the PG has been reported as 8830 cubic kilometers (Michael Reynolds 1993). The mean depth of this gulf is nearly 38 m, and the evaporation rate dominates the water loss in this shallow area. Besides, almost half of the desalination plants are located inside this gulf. Water exchange through the Strait of Hormuz and water circulation within the PG controls the hydrodynamic currents and salinity dispersion. The water circulation in the PG is mainly influenced by atmospheric forces, tides, river discharges, and water flow from the Strait of Hormuz. The north wind only affects the surface currents down to a depth of 10 m, and its impact on the deeper currents in the PG is very limited (Kamranzad 2018). The current enters the PG along the north coast

✉ Hassan Akbari
akbari.h@modares.ac.ir

Samad Rasoulpour
samad.rasoulpour@modares.ac.ir

[1] Department of Civil and Environmental Engineering, Tarbiat Modares University, Tehran, Iran

(Iranian coasts) from the Strait of Hormuz and moves to the northwest of the PG with a speed of more than 10 cm per second. Then, it moves southeastward in the southern part of the PG. The pressure gradient has a greater share in creating these currents than the north wind (Hunter 1983). The hydrodynamic conditions of the region are strongly related to the bed roughness (Afshar-kaveh et al. 2016). The increase in barometric pressure associated with the north wind occurs after a gradual decrease in water level. During the north wind event, surface currents in the northern PG intensify to their maximum speed. The maximum current speed occurs along the northwest coast of the PG and is about 15 cm per second. Unlike the surface currents, the currents in the middle and lower layers are less affected by the north wind (Li et al. 2020).

The water comes from the Indian Ocean, and continuous water circulation controls the salt content and the salinity stability of the Gulf (Ibrahim et al. 2020). Water with a lower salinity than the Indian Ocean enters the PG through the Strait of Hormuz. The current first enters the northern PG along the Iranian coast. A portion of these currents then exit the PG through the Strait of Hormuz along the southern coast. Evaporation of water in shallow areas along the coast of the PG increases water density, and this heavy water returns to the Indian Ocean as a sub-surface current through the Strait of Hormuz (Chow et al. 2019). The Gulf receives massive discharges of heated water from over 55 desalination plants, power stations, and heavy industrial facilities (Al-Mutaz 1991). While the effects of these discharges are sometimes assessed locally, they are not evaluated on a Gulf-wide basis (Sheppard et al. 2010). Some studies reported that desalination has little long-term effect on the mean salinity of water due to the buffering effect of the Indian Ocean, while evaporation is a key factor in both the hydrodynamics and surface hydrology of the PG (Elhakeem et al. 2015). In addition, the salinity levels in the PG exhibit significant variations in both space and time. Very high salinity values are produced in shallow areas west of Qatar and possibly in marshes near the southern coast. The water probably dilutes considerably before reaching the main basin of the gulf (Swift and Bower 2003).

Considering the existence of a warm and dry climate in the PG region, very hot summers and dry winds in winter, and the entry of clean water by rainfall of 0.15 m/y and river flows of 0.15—0.19 m/y, water salinity in most parts of the PG is more than 39 psu and even in southern areas of the Gulf where there is no running water, the salinity of 70 psu has been observed (Elhakeem and Elshorbagy 2013). Rapid growth has been fueled by population growth and changing climatic conditions, such as decreased or altered rainfall patterns. This has caused many communities to experience water shortages (Gray et al. 2011). Desalination plants use about 2 percent of the water that evaporates annually from the PG's surface. By the end of this century, new plants may increase this water use by five times (Paparella et al. 2022). The temperature rises in the PG due to climate change and coastal effluent discharge is spatially confined near the discharge locations (Elhakeem and Elshorbagy 2015). Due to its isolation from the Indian Ocean, the Gulf is a unique ecological entity. The number and size of desalination plants necessitate consideration of the impact of individual or multiple plants on the Gulf ecosystem as a whole (Höpner and Windelberg 1997). The use of seawater by desalination plants results in the production of thermal effluents that are typically 5 degrees Celsius warmer than the surrounding water. Additionally, the effluents contain residual chlorine, which is used to prevent fouling. The impact of this residual chlorine on seawater is not well understood and requires further investigation, particularly considering the Gulf's unique climatic conditions (Khan and Al-ajmi 1998). Some studies have investigated the local effect of desalinations either at outfall (Akbari and Ebrahimi 2016) or intake (Rahmani Firozjaei et al. 2023) locations, while some others have studied the regional effects (Paparella et al. 2022). The second approach, i.e., investigating the regional effects of desalination plants on the PG's salinity, is the primary concern of this study due to the semi-enclosed geometry, high salinity, and importance of this gulf.

Despite the studies about the desalination plant impacts, there remains a significant gap in understanding the long-term, cumulative general and local effects on the PG's salinity under different development scenarios of desalination plants. Since limited studies have been done to investigate the long-term functionality of desalination plants and their environmental effects on the PG salinity, this study aims to fill this gap by:

- Investigating the annual flow pattern and water exchange process within the PG, and finding the route of effluent discharges in this region.
- Modeling the 3D residual currents and salinity pattern in different depth layers of the PG.
- Evaluating the long-term impact of existing and proposed desalination plants on the PG's salinity.
- Assessing the relative contributions of natural factors (evaporation, water exchange) and human activities (desalination plants) in salinity changes.
- Detection local areas and vulnerable regions within the PG sensitive to rising salinity levels as a result of desalination plant developments.

As an important factor in decision-making for a sustainable development, the ultimate objective of this study is to evaluate the feasibility and potential impact of desalination plants on the PG's environmental conditions. The main challenges of this study were preparing a well-calibrated 3D flow

model and proper introducing the desalination parameters in the numerical model. In addition, providing integrated annual results in different layers based on the 3D results in an unstructured mesh was a challenging effort too. Based on the results, it can be concluded that although the overall salinity impact of desalination plants on the PG's environmental condition is negligible; special attentions should be paid to the possible significant regional and local impacts. Some areas are not suitable for establishing new desalination plants, while some other areas can face a potential risk even by new plants in distant regions. This research provides valuable insights for international engineers and managers, highlighting the importance of considering a comprehensive development plan taking into account the regional impacts and the interaction between available and future desalination plants. Such a general plan should pay special attention to the detected sensitive regions in this study.

In the following, the methodology and governing equations are presented at first, and then, the hydrodynamic and the transfer numerical models are validated in two separate sections. Afterward, the results are discussed in Sect. "Results and discussion," and at the end, the main findings are summarized in the conclusion section.

Materials and methods

The methodology of this study is presented in Fig. 1. A 3D numerical model was applied here to study the hydrodynamic and salinity conditions of PG in relation to the development of desalination plants. The governing equations and then the model inputs are presented in this section. After that, the models are verified and compared to available and measured hydrodynamic and environmental data.

Governing equations

The main governing equations are Navier–Stokes and transfer equations used for modeling hydrodynamic, temperature, and salinity levels. However, there are also some accessory sub-equations necessary to support the hydrodynamic or transfer equations. The effects of different sources such as wind momentum, rain and evaporation, rivers, and heat exchanges are included in these accessory equations. In the following, only the main hydrodynamic and transfer equations are presented, and other sub-equations are referred to the manual of the utilized software and the previous studies (Munk and Anderson 1948; Dhi 2013).

Navier–Stokes equations

The applied model solves the shallow water equations denoted by the 3D incompressible Reynolds Averaged Navier–Stokes equations as continuity and momentum equations (Dhi 2013) as.

Continuity equation:

$$\frac{\partial u}{\partial x} + \frac{\partial v}{\partial y} + \frac{\partial w}{\partial z} = S \tag{1}$$

Two-dimensional horizontal momentum equations for x and y components, respectively:

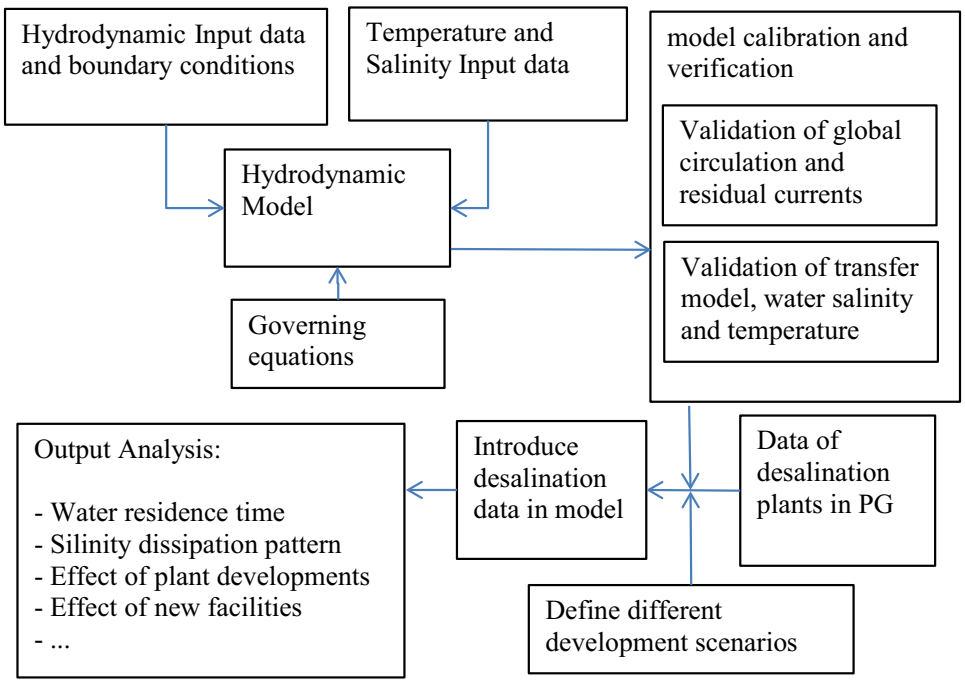

Fig. 1 Flowchart illustrating the methodology of this study

$$\frac{\partial u}{\partial t}+\frac{\partial u^2}{\partial x}+\frac{\partial vu}{\partial y}+\frac{\partial wu}{\partial z}=fv-g\frac{\partial \eta}{\partial x}-\frac{1}{\rho_0}\frac{\partial p_a}{\partial x}-\frac{g}{\rho_0}\int_z^\eta\frac{\partial \rho}{\partial x}dz-\frac{1}{\rho_0 h}\left(\frac{\partial s_{xx}}{\partial x}+\frac{\partial s_{xy}}{\partial y}\right)+F_u+\frac{\partial}{\partial z}\left(v_t\frac{\partial u}{\partial z}\right)+u_sS \tag{2}$$

$$\frac{\partial v}{\partial t}+\frac{\partial uv}{\partial x}+\frac{\partial v^2}{\partial y}+\frac{\partial wv}{\partial z}=fu-g\frac{\partial \eta}{\partial y}-\frac{1}{\rho_0}\frac{\partial p_a}{\partial y}-\frac{g}{\rho_0}\int_z^\eta\frac{\partial \rho}{\partial y}dz-\frac{1}{\rho_0 h}\left(\frac{\partial s_{yx}}{\partial x}+\frac{\partial s_{yy}}{\partial y}\right)+F_v+\frac{\partial}{\partial z}\left(v_t\frac{\partial v}{\partial z}\right)+v_sS \tag{3}$$

The horizontal stresses in the x and y directions can be expressed as:

$$F_u=\frac{\partial}{\partial x}\left(2A\frac{\partial u}{\partial x}\right)+\frac{\partial}{\partial y}\left(A\left(\frac{\partial u}{\partial y}+\frac{\partial v}{\partial x}\right)\right) \tag{4}$$

$$F_v=\frac{\partial}{\partial y}\left(2A\frac{\partial v}{\partial y}\right)+\frac{\partial}{\partial x}\left(A\left(\frac{\partial u}{\partial y}+\frac{\partial v}{\partial x}\right)\right) \tag{5}$$

It should be noted that the well-known k-ε turbulence model is solved to obtain turbulence viscosityv_t. In addition, the fluid is taken to be incompressible, so pressure does not affect water density, and only temperature and salinity do, according to the equation of state (UNESCO 1981):

$$\rho=\rho(T,s) \tag{6}$$

2–1-2- Transfer equations (temperature and salinity) The transfer of temperature and salinity follows the following diffusion and displacement equation:

$$\frac{\partial T}{\partial t}+\frac{\partial uT}{\partial x}+\frac{\partial vT}{\partial y}+\frac{\partial wT}{\partial z}=F_T+\frac{\partial}{\partial z}\left(D_v\frac{\partial T}{\partial z}\right)+\hat{H}+T_sS \tag{7}$$

$$\frac{\partial s}{\partial t}+\frac{\partial us}{\partial x}+\frac{\partial vs}{\partial y}+\frac{\partial ws}{\partial z}=F_s+\frac{\partial}{\partial z}\left(D_v\frac{\partial s}{\partial z}\right)+s_sS \tag{8}$$

In the above equation, the terms of temperature and salinity diffusion are as follows:

$$(F_T,F_s)=\left[\frac{\partial}{\partial x}\left(D_h\frac{\partial}{\partial x}\right)+\frac{\partial}{\partial y}\left(D_h\frac{\partial}{\partial y}\right)\right](T,s) \tag{9}$$

It should be noted that the other equations (such as one related to evaporation, ocean-atmospheric interaction, and heat exchange) are also solved and involved in the hydrodynamic and transfer modules. Meanwhile, since these equations are well-known to mathematical researchers (refer to Rodi 2017; Smagorinsky 1963; Wu 1980; Iqbal 1983), the main equations are only presented here for a better presentation and discussing the more important issues. The model inputs, boundary conditions, and the validation of the results are presented with more detail in the following sections.

Boundary conditions and input parameters

The finite volume method is used to solve the water hydrodynamics equations that control the computational domain. It splits the domain into three dimensions with connected and non-overlapping cells. This study did three-dimensional modeling and used an irregular grid in horizontal layers and a regular grid in vertical direction. The grid had 5083 nodes and 9233 elements. Ten vertical sigma layers were chosen, and the largest element areas in the coastal and offshore regions of the PG were 38.62 and 77.24 km^2, respectively. As shown in Fig. 2, finer meshes are applied near the shorelines where desalination outfalls are located in shallow depths.

Locations of desalination plants are presented in Fig. 3 (according to the data provided by the Iranian Ministry of Energy 2021). The effluent discharge of each desalination plant depends on the desalination technology. As indicated in Table 1, the salinity of seawater varies depending on the utilized water desalination technology (Elhakeem and Elshorbagy 2015). In this table, MSF, MED, and RO stand for multistage flash, multi-effect desalination, and reverse osmosis technologies, respectively. It should be noted that many of the former plants usually in the southern part of the PG (66 percent) employ the MSF technology, while the recent ones employ RO technology. In this study for hybrid technologies that employ two distinct methods, the maximum value has been considered. Based on the available data, the total capacity of desalination plants is assumed as 8.25 BCM/y (Billion m^3/y) with the brine outputs of 12.24 BCM/y.

A full-slip boundary condition is applied along the coastlines to ensure that the speed perpendicular to the coast is zero. In addition, data from HYCOM model are applied at open boundaries using the Flather boundary condition to link the water height and flow speed at the edge (Oddo and Pinardi 2008). The explicit numerical solution requires a small time step for stability reasons, as the Courant number must be below one. As discussed by (Ranjbar et al. 2020), a high-order method is needed for the temperature/salinity module to ensure sufficient accuracy and consistency with the measurements; however, the hydrodynamics equations can be solved with a low-order method.

The primary inputs of numerical models are climatic conditions including the data of wind, air temperature, evaporation, and precipitation. The data related to water level, salinity, and water temperature (both for boundary conditions and initial conditions) were extracted from HYCOM model. The geographical accuracy of these data is 0.08 by 0.08 degrees, and the time step of data is one hour. In addition, the study used ECMWF-Era5 data from the Copernicus Data store (CDS) with a spatial resolution of 0.25 × 0.25 degrees and a temporal resolution of one hour for all wind,

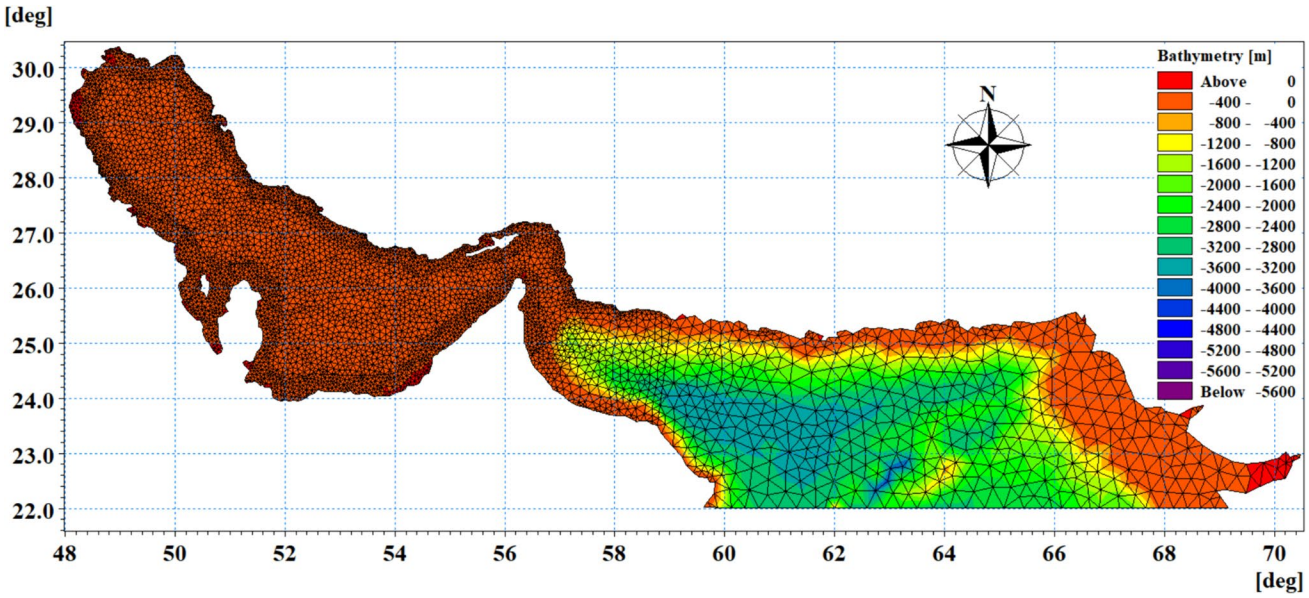

Fig. 2 Horizontal meshing of the computational domain

Fig. 3 Map of water desalination plants' sites

Table 1 Brine production by desalination technologies and increase in salinity and temperature

	MSF	MED	RO
Volume of saline feed water per m3 of freshwater	4	3	2 ~ 2.5
Volume of brine effluent per m3 of freshwater	3	2	1 ~ 1.5
Recovery (%)	25	33	50
Salinity increase to ambient (ppt)	10	15	44.8
Temperature increase to ambient (° C)	10	10	1

evaporation, and air temperature data. The results showed that evaporation was higher in winter than in summer due to the more significant influence of wind speed than temperature on evaporation rate (Michael Reynolds 1993). In the literature, the evaporation and precipitation rates in PG have been reported as 1.4 to 2.4 m/y and 0.07 to 0.15 m/y, respectively. These values show the importance of evaporation in this gulf. In this study, according to the PG area, the net evaporation rate (i.e., evaporation minus precipitation) is 1.83 m/y or 437.37 BCM/y.

The bathymetric measurements for the PG and Sea of Oman were sourced from GEBCO (2022). In addition, the Ports and Maritime Organization provided data on the depth of the bed of the PG and Oman Sea. Bed roughness was selected as 0.05 based on a sensitivity analysis. In addition, the river freshwater budgets from 0.07 to 0.46 m/y were reported in the literature. In this study, the data of main rivers, including flow rate, salinity, and temperature are extracted from previous studies (Elhakeem et al. 2015; Kämpf and Sadrinasab 2006; Michael Reynolds 1993; Pous et al. 2004; Campos et al. 2020) and implemented in the model as different sources with lower salinities (6 to 11 psu according to these references). Based on the results, the mean river discharges in a year are approximately 52.6 BCM/y or 0.22 m/y.

The study used the winter season as the starting point for modeling, as the water column temperature was relatively uniform during this season. The initial conditions for water level, salinity, and temperature in three dimensions were obtained from the HYCOM hydrodynamic model with a spatial resolution of 0.08×0.08 degrees for the PG and Oman Sea domain. The initial flow velocities were set to zero for all three components, and the simulation ran for 8 years until it reached a steady state after a cold start period. The model output showed minimal variation between consecutive years in the final year of modeling, as indicated in Figs. 4 and 5. In addition, the water salinity becomes stable after three years while the temperature stabilizes very fast.

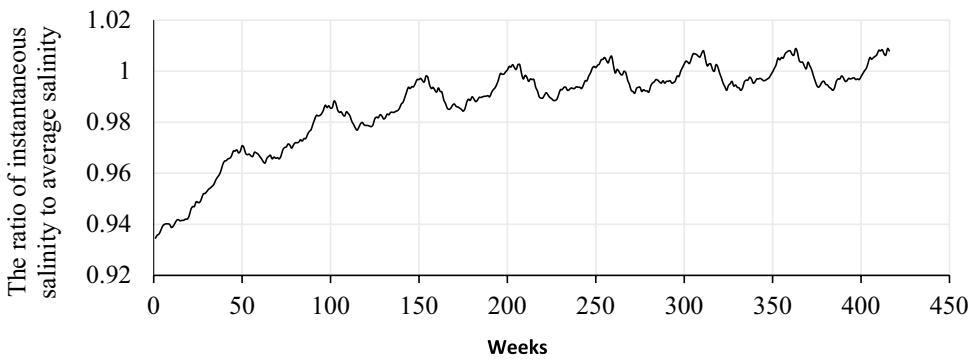

Fig. 4 Instantaneous salinity ratio to stable salinity of the PG surface water Si/Ss during 8-year simulation. The horizontal axis indicates the number of the weeks since the beginning of 2012

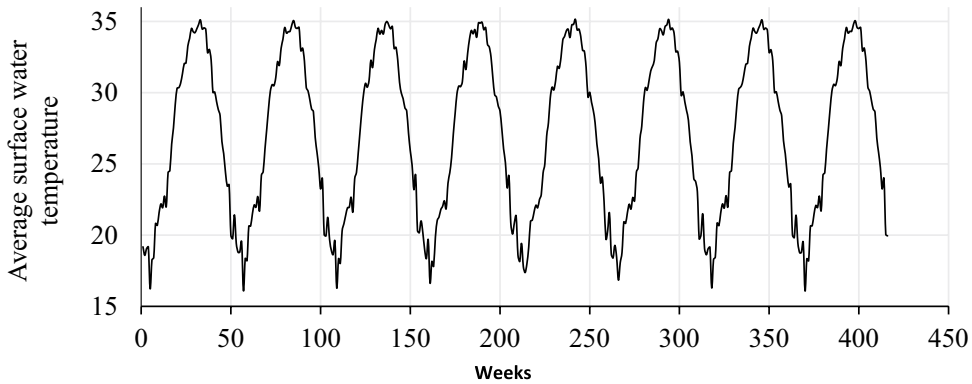

Fig. 5 Average surface water temperature of the PG during 8-year simulation. The horizontal line indicates the number of the weeks since the beginning of 2012

Validation of the Numerical Model

In this section, the model results are verified and compared to available measured or simulated data. The validations of the hydrodynamic and transfer models are presented in the two subsequent sections, respectively.

Validation of hydrodynamic model

Tidal levels and local currents

The current model's ability to reproduce tidal heights and speeds at different points on the PG surface is assessed. To avoid the effect of other parameters on the tidal level and currents, the simulation is performed by implementing only the tidal data at the model boundaries. For this purpose, the global tidal prediction model that relies on satellite data and data analysis based on ten major tidal components was utilized with a spatial accuracy of 0.125×0.125. For comparing the results, the TPXO database (Lee and Kaihatu 2018) which provides tidal forecasting at any location for a week is applied. The comparisons between the TPXO data and the simulated tidal currents and levels are presented in Table 2.

Root mean square error (RMSE) and Pearson correlation coefficient (R) were applied to assess the simulation accuracy. The average RMSE for tidal elevation and velocity was 0.144 m and 0.0755 m/s, respectively, based on six points in the PG. Moreover, the prediction data and simulation outcomes had an average correlation coefficient of 0.95 for tidal elevations and 0.844 for velocities. These outcomes confirm the ability of the utilized numerical tool to model tidal current as the most important parameter in dissipating the effluent discharges in the PG.

Validation of global circulation and residual currents

The water circulations and residual currents are the most crucial factors in moving the pollutions out of the PG through the Strait of Hormuz. The simulated residual currents in the Strait of Hormuz (in the longitudinal coordinate of 56 degrees east) are compared in Fig. 6 with the Yao's study (Yao 2008) for the months of February, May, August, and November. The presented data illustrate the velocity of flow in the u-component direction. Negative velocities indicate flow into the PG, while positive velocities represent flow out of the PG. Figure 6 illustrates that water enters the PG from the northern shores of the Strait of Hormuz. After circulating within the PG, it exits through the Strait of Hormuz in layers near the bed. This flow pattern is compatible with the findings of (Chow et al. 2019). In addition, the residual currents on the northern coasts are significantly faster than those on the southern coasts. Based on the results, the discharge of the freshwater incoming from the Oman Sea to the PG is almost 0.228 sv, while the discharge of outgoing salted water is 0.215 sv ($1\text{sv} = 10^6\ \text{m}^3/\text{s}$). Therefore, the net discharged water through the Strait of Hormuz is nearly 0.013 sv (equal to 411.08 BCM/y, or 1.72 m/y). According to the net evaporation rate in this shallow gulf, most of this incoming water will be compensated with evaporation which shows the importance of evaporation in this area. However, it should be noted that if the evaporation rate or any climate condition changes in the future (evaporation exceeds the existing values, for example), a new equilibrium condition may be established as reported by (Ibrahim et al. 2020), and the incoming water to the gulf will be justified in accordance with the mean water level in free seas.

In addition to the residual currents in the Strait of Hormuz, the water circulation pattern inside the PG is another important factor that affects the route of pollutions. Hosseinibalam et al. (2011) employed a hydrodynamic ecological model coupled with the oceanic continental shelf to predict water circulation in the PG. This model considered the effects of wind stress and surface salinity temperature flux on the circulation patterns. The study's findings indicated a positive correlation between the outflow rate from the bed of the PG and the surface flow entering the Gulf. They further demonstrated that the heat flux plays a critical role in shaping the water circulation of the PG. In addition, the wind stress was observed to create a surface current with a

Table 2 Comparison of the simulated speed and tidal levels with TPXO prediction models

Point	Latitude (degrees)	Longitude (degrees)	Comparison with tidal current speed		Comparison with tidal level	
			RMSE(m/s)	R	RMSE(m)	R
t1	29.86541	48.69130	0.09	0.81	0.13	0.97
t2	27.42151	50.69008	0.09	0.8	0.14	0.92
t3	25.85022	53.24636	0.08	0.95	0.1	0.94
t4	29.69636	50.15069	0.06	0.86	0.17	0.92
t5	27.63258	52.07376	0.05	0.79	0.13	0.97
t6	26.50688	54.32516	0.07	0.82	0.17	0.98
Average			0.07	0.84	0.14	0.95

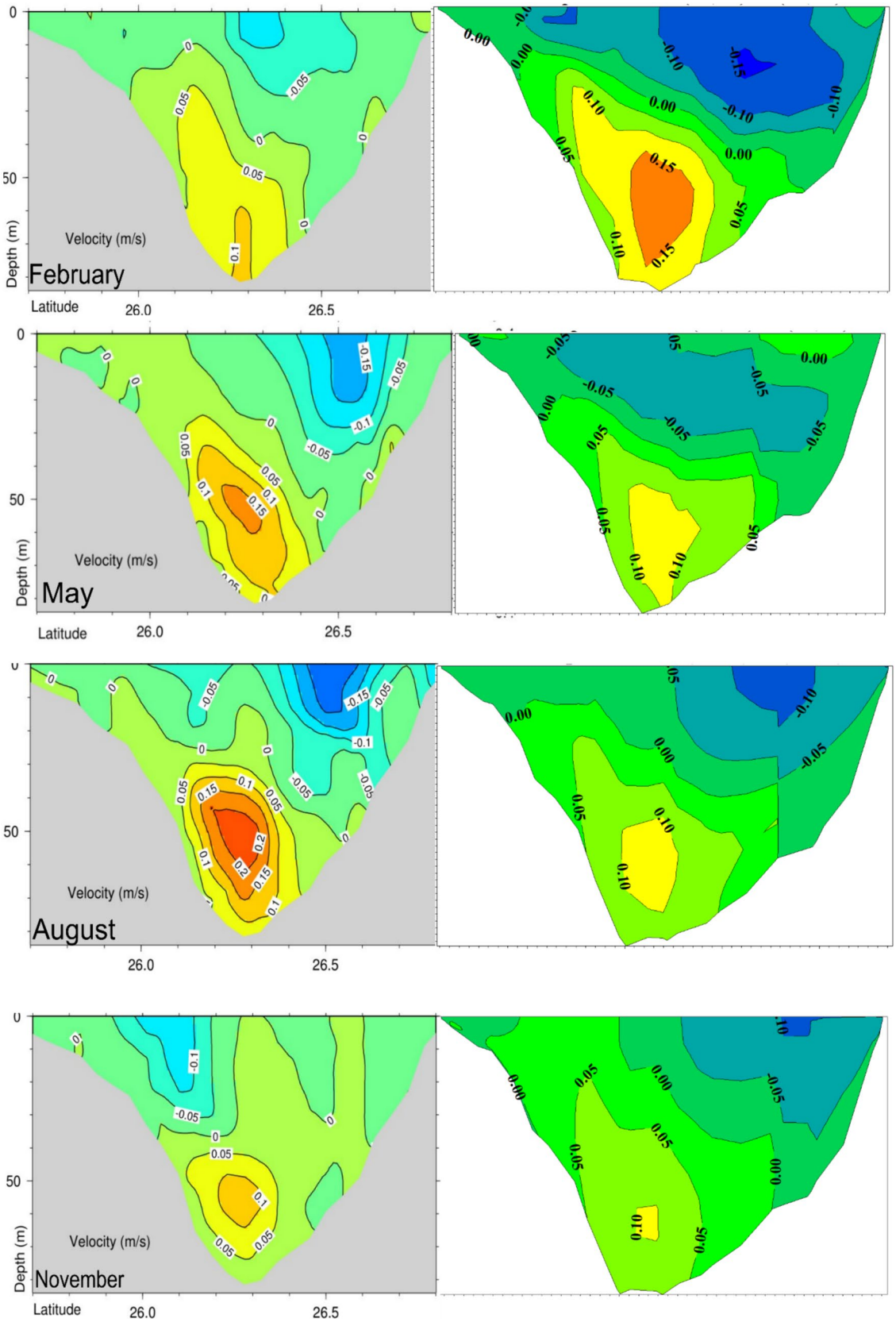

Fig. 6 Simulation (right) and Yao's studies (left); Comparison of residual current velocity U component in the Strait of Hormuz

velocity of 5 cm/s (Hosseinibalam et al., 2011). Later, Chow et al., (2019) investigated the water circulation in the PG and found that the region is influenced by water interchange with the Indian Ocean. Water with a lower salinity flows into the PG from the Indian Ocean through the Strait of Hormuz, labeled as T1 in Fig. 7. The northern inflow of the PG originates from the Indian Ocean and enters the Gulf, with a minor fraction of this inflow exiting the Strait of Hormuz along the southern Gulf coast, denoted as T2. Water evaporation in the shallow areas along the Gulf shores increases water density, causing dense water to flow back to the Indian Ocean as a subsurface current through the Strait of Hormuz, labeled as T3. That study also found that water may remain in the shallow areas along the coasts of Arab countries for 2–3 years and not participate in the general circulation of the PG (Chow et al. 2019). The flow pattern simulated in this study (presented in Fig. 6) also confirms the same pattern of flow exchanges at the Strait of Hormuz that is the freshwater entering from the shallower northern areas and exiting from the deeper areas.

In addition, some researchers have studied the global pattern of currents in the PG. Figure 8 shows a comparison of the modelling results of residual currents (Fig. 8c) with the findings of Ranjbar et al. (2020) and Michael Reynolds (1993). The current research agrees with previous studies in that the water flow from the Strait of Hormuz enters the PG at a relatively high speed. This current travels from the northern coast to the northwest of the PG and from the southern coast to the southeast. Several counterclockwise vortices are formed along the way. In addition, there are weak currents with variable directions in the northern part of the PG.

As presented in Fig. 9, the routes of floating buoys measured during the Mt. Mitchell ship research (as reported in Reynolds's article) are also nearly compatible with the global pattern of the obtained circulations. The end of the trackers is indicated by an arrow in this figure, and the number of days spent on the route is also depicted. Two buoys 9450 and 9451 were moved outside the PG.

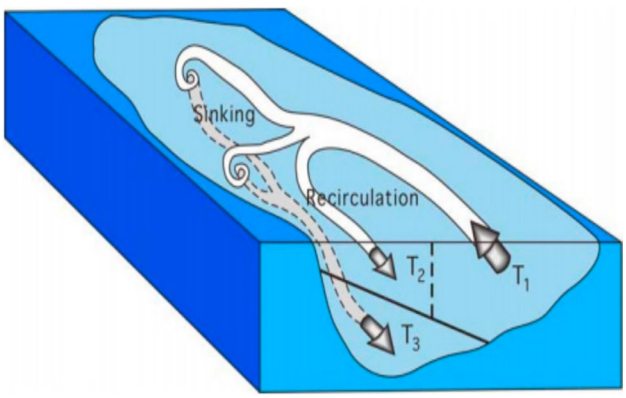

Fig. 7 Schematic of circulation through the Strait of Hormuz (Chow et al. 2019)

To compare the results of this research with the previous studies, the main hydrodynamic outcomes are also presented in Table 3 including the input and output water exchanges to the semi-enclosed PG. All the data are divided by the area of PG to be comparable with the same unit of (m/y), i.e., the annual change in mean water elevation. In this table, the incoming and outgoing water through the Strait of Hormuz are depicted by Qin and Qout, respectively, and Qnet stands for the net value of incoming freshwater. The amounts of evaporation, rainfall, and their difference as net evaporation and river discharges are also presented in the next columns of this table. In addition, the values obtained in this study are reported in the last row of the table and it is clear that the results are completely in the range of the previous findings. This compatibility confirms the general quality of the simulated data too.

Validation of transfer model

Validation of water salinity

In 1992, following the PG War, the research vessel Mt. Mitchell conducted a study on the impact of oil spills on the water quality of the PG. The ship collected salinity data from various locations across the gulf (Michael Reynolds 1993). The locations of these data points are shown in Fig. 10. The 3D salinity stratification in the PG can be largely inferred from the vertical salinity profiles at two sections presented by red line in this figure: section C in the Strait of Hormuz, where the water exchange between the PG and the Sea of Oman occurs, and section I in the central part of the PG at a depth of 80 m.

The simulated vertical salinity profiles at sections C and I are presented in Figs. 11 and 12 alongside the measured data by Reynolds. A general comparison confirms that the model used has successfully simulated water flow and salinity stratification in the PG. These results indicate that low-salinity water from the Gulf of Oman enters the PG at the surface and extends along the Iranian coast to compensate for evaporation in the PG. Saline water is then directed through the bottom and along the southern coast of the PG toward the Strait of Hormuz. Therefore, at sections C and I, water at the surface is low in salinity and increases in salinity with depth.

In the winter, there is a significant difference between the surface water salinity and near-bottom water salinity in section C. The surface water salinity in the northern part of the Strait of Hormuz is 37 psu, and this value increases to 40 psu at the bottom. This indicates that low-salinity water enters the PG from the surface, and denser water (water with lower temperature and higher salinity) moves from the depths of the Strait of Hormuz to the Gulf of Oman. In the summer,

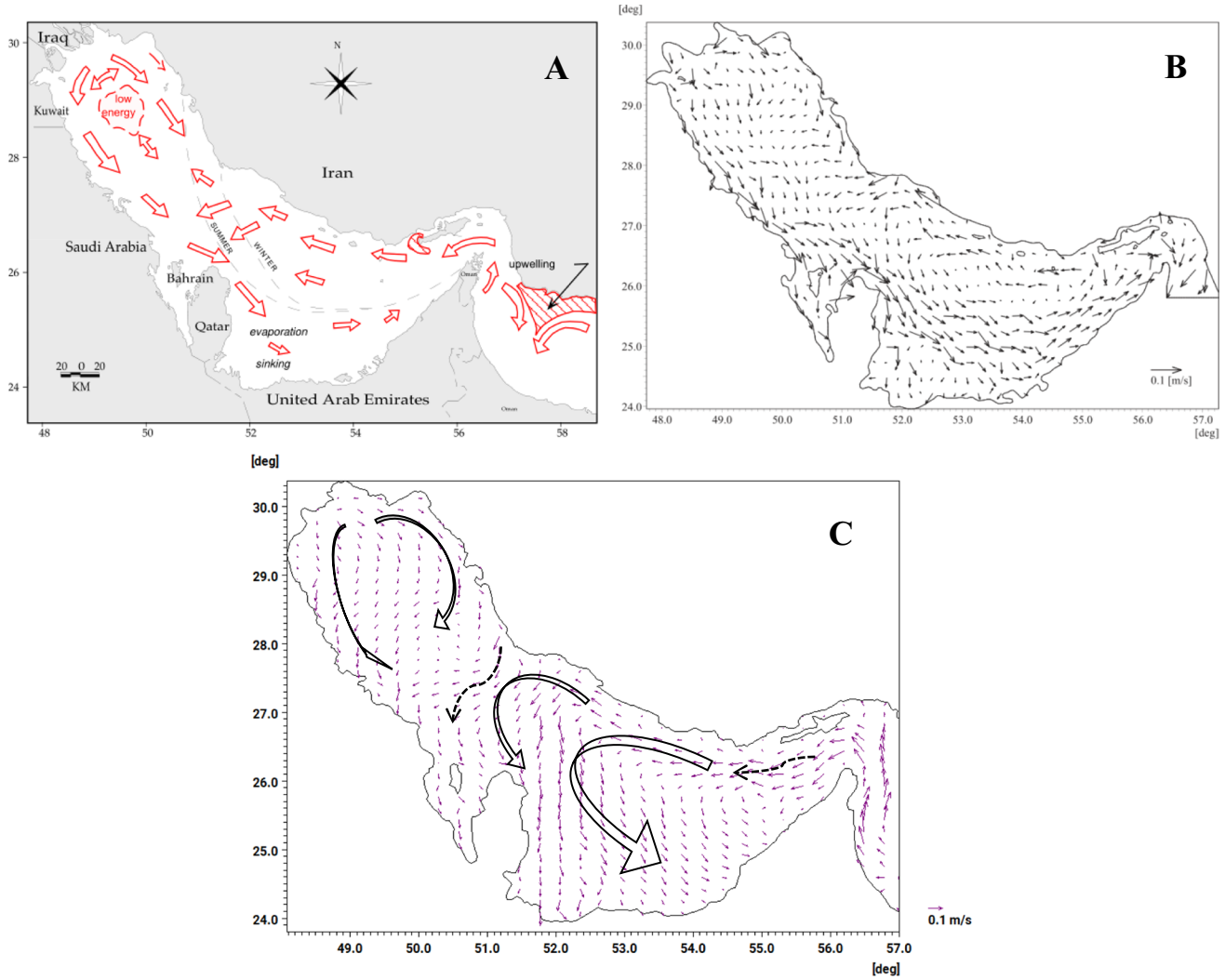

Fig. 8 General circulation of surface currents in PG, A: Michael Reynolds (1993); B: Ranjbar et al. (2020); C: This research

the vertical salinity profile stratification is almost inclined to the southern part of the Strait of Hormuz. The distribution pattern and level of the water salinity in section C differs slightly from the summer to the winter. The water salinity is approximately 0.5 psu higher in the winter than in the summer. This issue can be clearly observed in simulation results.

During the winter, water salinity stratification is observed to be vertical within the section I. A noticeable difference between the northern and southern regions' salinity levels is evident across all the graphs presented in Fig. 12. During the summer months, the water salinity level in section I changes from 38 psu along the northern coastline to almost 43 psu along the southern coastlines. It reaches nearly to 41.5 psu in the deeper central regions between the two coastlines. However, there exists a variance of 2–3 psu between the measurements and the simulation results, especially near the southern coasts.

Validation of water temperature

Water temperature is not the primary concern of this study rather than salinity. However, to be sure about the model, it is also verified here since it can affect the water density and hydrodynamic model. Similar to the salinity, the numerical results are compared with those provided by Reynolds (1993) in Fig. 13. Although the values are not the same due to the fact that they are not for an exact year, the trends of heat distributions along depth are in good agreement with the available data in different seasons. This compatibility confirms the model's ability in heat modeling.

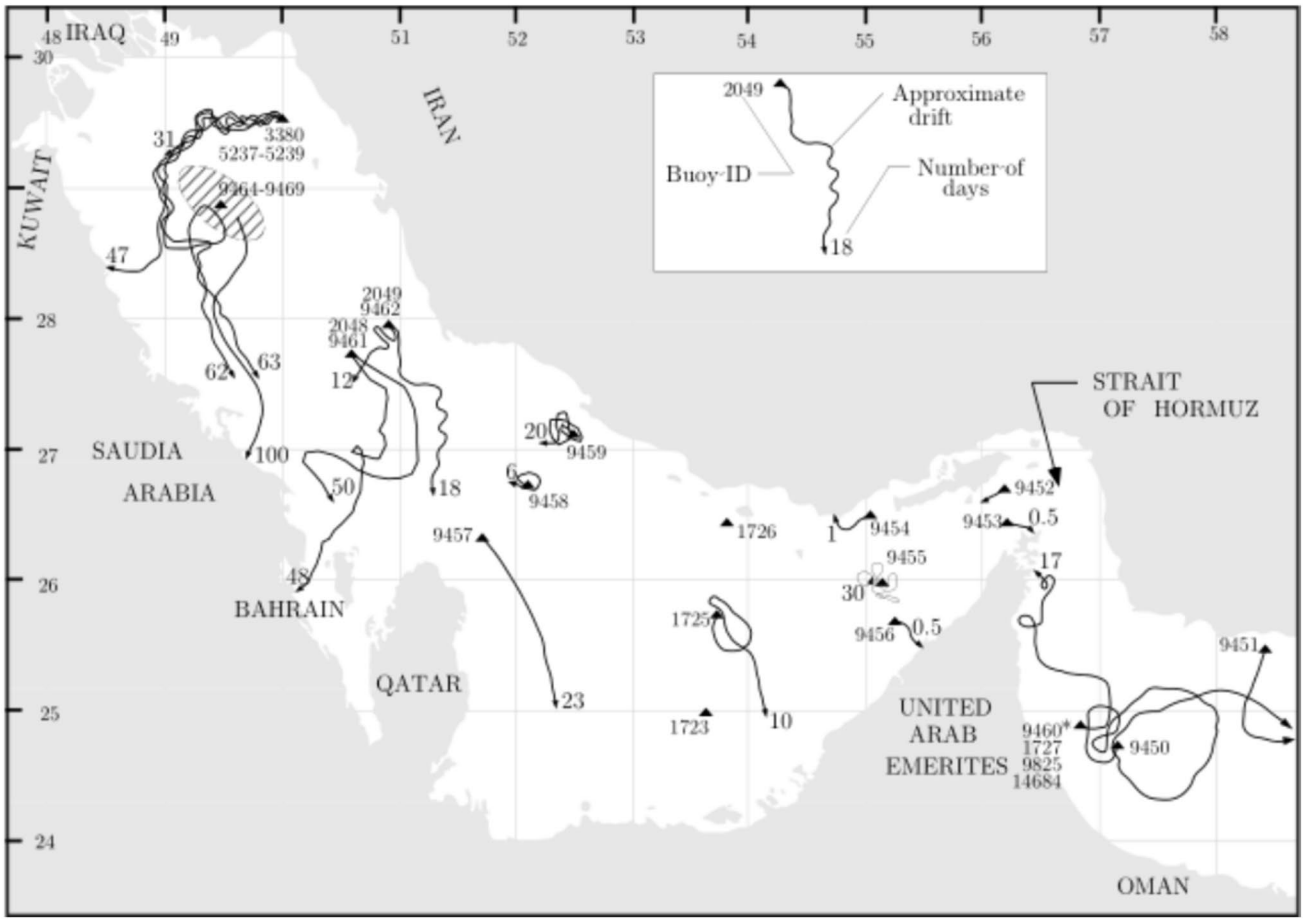

Fig. 9 Tracking of the drifter buoys based on (Michael Reynolds 1993)

Table 3 Comparison between the hydrodynamic results and previous studies

Reference study	Qin (m/y)	Qout (m/y)	Qnet (m/y)	Evap. (m/y)	Rainfall (m/y)	Net Evap. (m/y)	Q river (m/y)
(Mahpeykar and Khalilabadi 2021)				1.45–2.42		1.20–1.43	
(Ibrahim et al. 2020)				1.84			
(Xue and Eltahir 2015)	33.70	32.10	1.60	1.84	0.08–0.15	1.76	0.21
(Pous et al. 2015)	30.35	27.71	2.64	2.00	0.15	1.85	0.18
(Pous et al. 2004)	27.71	22.43	5.28	1.44–2.00	0.07–0.10	1.37–1.90	0.15–0.46
(Paparella et al. 2022)						1.53	
(Campos et al. 2020)		19.8–34.3	1.61	1.51–5.1	0.07–0.1	1.44–5.0	0.44
This study	30.12	28.40	1.72	1.91	0.08	1.83	0.22

Results and discussion

Some results of this research, including the water circulation pattern, the residual currents, exchange waters, and the dissipation pattern of salinity and temperature within the PG were presented in the previous section, along with the results of other studies to validate the model. On the other hand, water demand and the number of desalination plants are increasing as predicted by different researchers. For instance, Paparella et al. 2022 predicted that the capacity of desalination plants in the PG will be increased from 8.25 BCM/y in 2022 to 14.4 and 33.5 BCM/y in 2030 and 2050, respectively. Therefore, in this section, the salinity of the PG is investigated in two cases: creating new facilities or increasing the capacity of the existing desalination plants. For this purpose, the natural refining capacities of the PG and the residence times in different areas of PG are

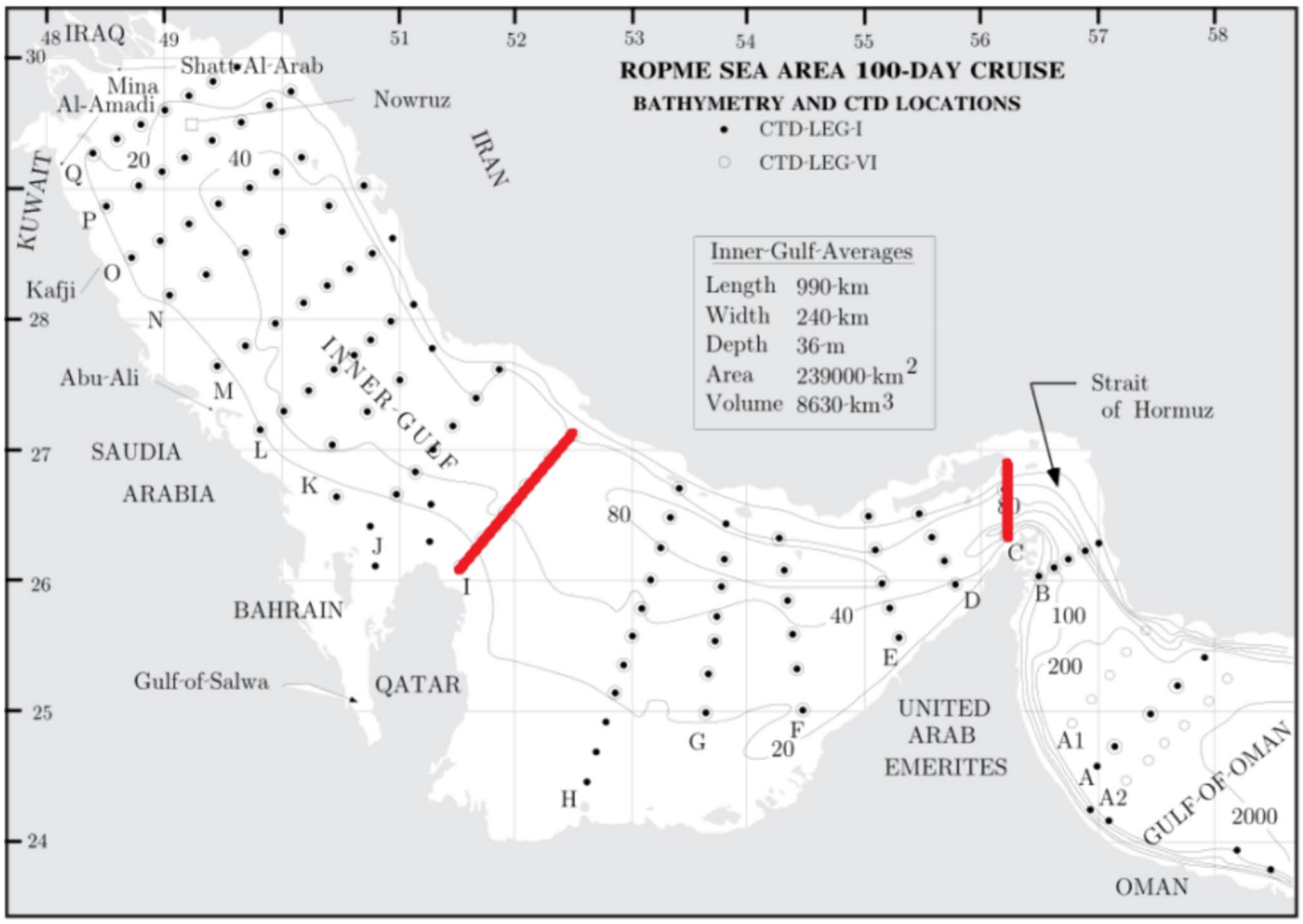

Fig. 10 The sections where salinity profiles were measured and reported by Michael Reynolds (1993); Section C: right red line near the Strait of Hormuz; Section I: left red line at the middle of the PG

investigated at first. Then, two scenarios have been considered to investigate the effect of future developments on the total salinity of PG. For the first scenario, the capacities of the existing desalination plants are increased by 50 and 100 percent, and for the second scenario, the impact of constructing new big desalination plants in different areas of the PG is studied.

Water residence time in PG

The water residence time may be characterized as the duration required for the tracer substance to decrease to 1/e or 37% of its initial concentration (Thomann, 1987). An alternative methodology involves determining the water retention time within each computational cell by measuring the duration required for 95% of the tracer substance's concentration to be dispersed to adjacent cells (Sadrinasab and Kämpf 2004). According to (Ranjbar et al. 2020), the water residence time in the PG was calculated using the second definition. The results of their model indicated that the water residence time in the western and southern regions exceeded nine years. Utilizing the same definition (Alosairi, Imberger and Falconer, 2011) estimated the water residence time to be up to three years. Two calculated residence times by these researchers are presented in Fig. 14.

In the present study, the initial pollutant concentration in the PG region was doubled (100% increase in the existing salinity) in the stabilized transport module, and the residence time is then calculated for different points as indicated in Fig. 15. The results are presented for three depths (surface, middle, and bottom layers) in Fig. 16. The threshold line that represents 36.7% of the initial concentration, as per Thomann's (1987) approach, is also indicated in this figure. As depicted and anticipated, the concentration of pollution decreases at a more rapid rate at the points near the Strait of Hormuz than at the internal points.

To further investigate the results, the time series of pollutant concentrations at each point were studied in different depth layers (i.e., on the surface, middle layer, and near the bed). As illustrated in Fig. 17, the difference in pollutant concentration across vertical layers decreases, and the pollutant layer becomes more uniformly distributed in the

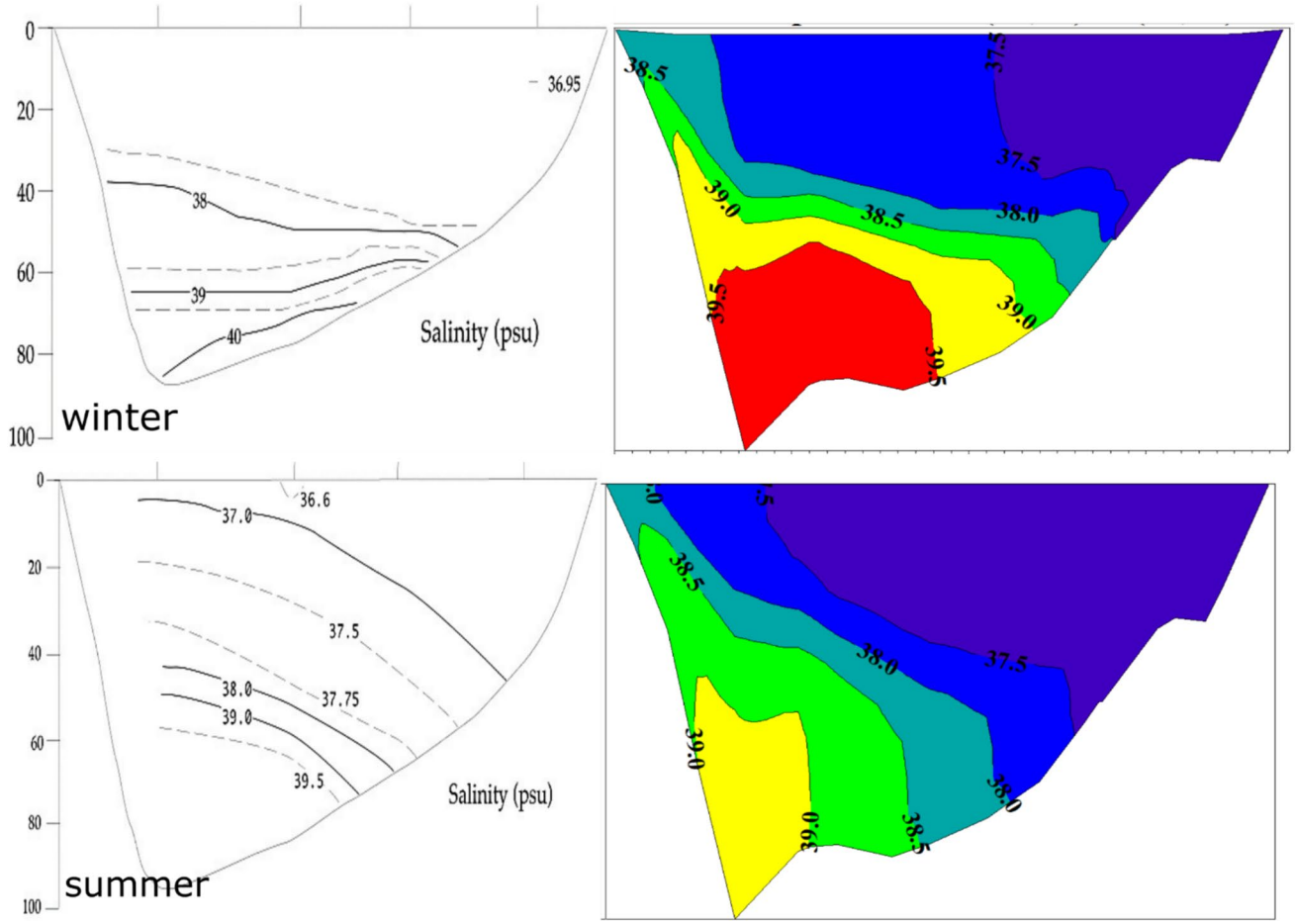

Fig. 11 The vertical salinity profile at section C; on the right: the simulation output, and on the left: the measurements by Reynolds (1993)

vertical direction as the distance from the Strait of Hormuz increases (from point S1 to S8).

At points S1 to S4, it takes between 26 and 45 months for water surface pollutants to decrease to 37% of their initial concentration. This time is 43 to 55 weeks for the middle layer and slightly longer for the layer near the bed. For these points which are relatively close to the Strait of Hormuz, the dissipation rates are minimal, especially in the lower layers, resulting in a significant increase in the residence time. Therefore, the concentration of water pollutants on the surface reaches a value below the threshold line in a shorter time than in the lower layers. The cause of this issue is that in deeper areas, such as points S1 to S4, the effect of wind force on the surface, in conjunction with tidal currents and differences in density gradients, accelerates the water flow on the surface. However, at shallower areas such as points S5 to S8, wind force acts more uniformly throughout the water column, and therefore, the residence time (which is 48 to more than 65 months) is nearly constant in depth. The calculated residence times at different points are summarized in Table 4.

To investigate the pollutant concentration at different depths of the PG, the remained pollutions after 5 years are presented in Fig. 18. This figure illustrates that the northwestern and southern regions of the PG are more susceptible to pollution, while the northern coasts and areas closer to the Strait of Hormuz are in better condition. According to Thomann's (1987) definition, the water retention time in this area is 3 to 4 years. The results also indicate that a significant portion of the northern coasts and central regions of the PG will be cleaned after 5 years. However, it takes more than 5 years for the northern regions of the PG and the regions near the Gulf of Bahrain.

Based on the data presented in Fig. 18, it is clear that the remained pollutions in different layers are generally the same, except in the eastern region of the Strait of Hormuz, where noticeable vertical changes can be observed. In the following, since the input water of desalination plants is usually fed from the bed layer, the trend of pollutant

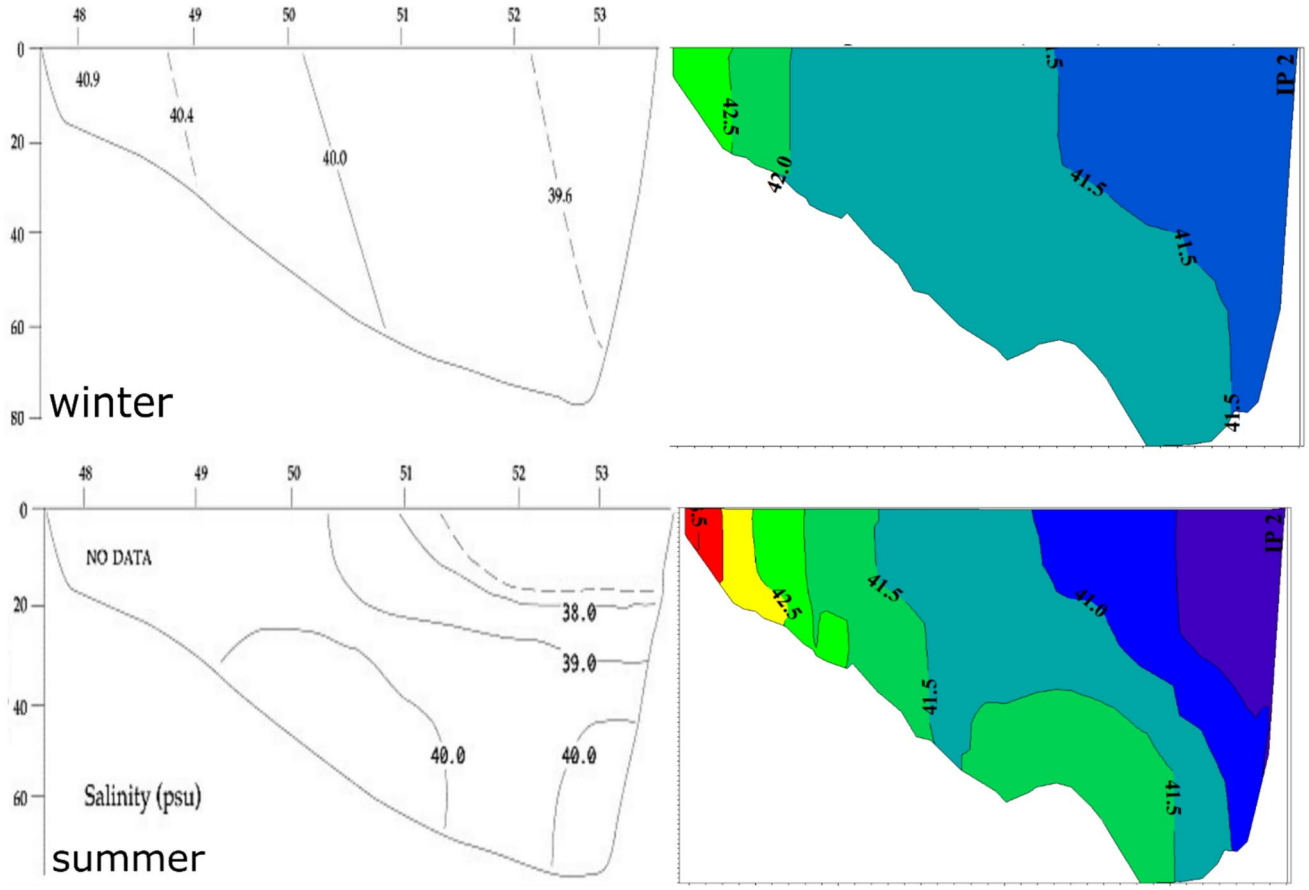

Fig. 12 Vertical salinity profile in section I; Right side: simulation output, and left side: measurement by Reynolds (1993)

concentration changes in the bed layer over time is shown in more detail in Fig. 19.

The effect of increasing the effluent discharge of desalination plants

Four scenarios have been taken into account to investigate the effect of existing desalination plants and their development as: I) the absence of all desalination facilities, II) presence of current desalination facilities, III) 50% increase in effluent discharge from existing facilities, and IV) 100% increase in effluent discharge from existing facilities. Figure 20 illustrates the variations in the mean surface salinity of the PG due to augmented effluent discharge from desalination plants under these four scenarios.

Compared to the state without any desalination brine, the averaged surface salinity has been increased by 0.02 psu due to the presence of existing desalination plants. Furthermore, a 50% increase in existing brine discharges increases the average salinity by 0.01 psu, while this increase remains consistent throughout the years. However, the difference between the third and the fourth scenarios (50% and 100% increase in brine discharge) is less than 0.01 showing a decreasing rate in excess salinity due to increasing the brine discharges.

To further investigate the impact of wastewater discharge on salinity levels in different areas of the PG, the average salinity difference between the first scenario (i.e., without desalination facilities) and other scenarios are calculated as ($\overline{SIM_i - SIM_1}$), and the results are presented in a two-dimensional horizontal format in Fig. 21. Based on this figure, the areas more susceptible to increases in water salinity can be identified. As shown in this figure, the seawater salinity rises generally along the southern shallow region, while the northern shorelines experience only a slight increase in salinity level. This is due to the nature of current circulation in the PG, as discussed in Sect. "Validation of global circulation and residual currents." Meanwhile, there are some vulnerable areas at the northern coast; one of them is located above the Qeshm Island where the current speed is high and big desalination plants exist. The situation of this area is discussed in more detail in the next section.

As shown in Fig. 21, the average increase in the salinity of the PG due to the presence of existing desalination is not physically sensible. The average value of salinity increase even in the southern parts with a worse condition is only

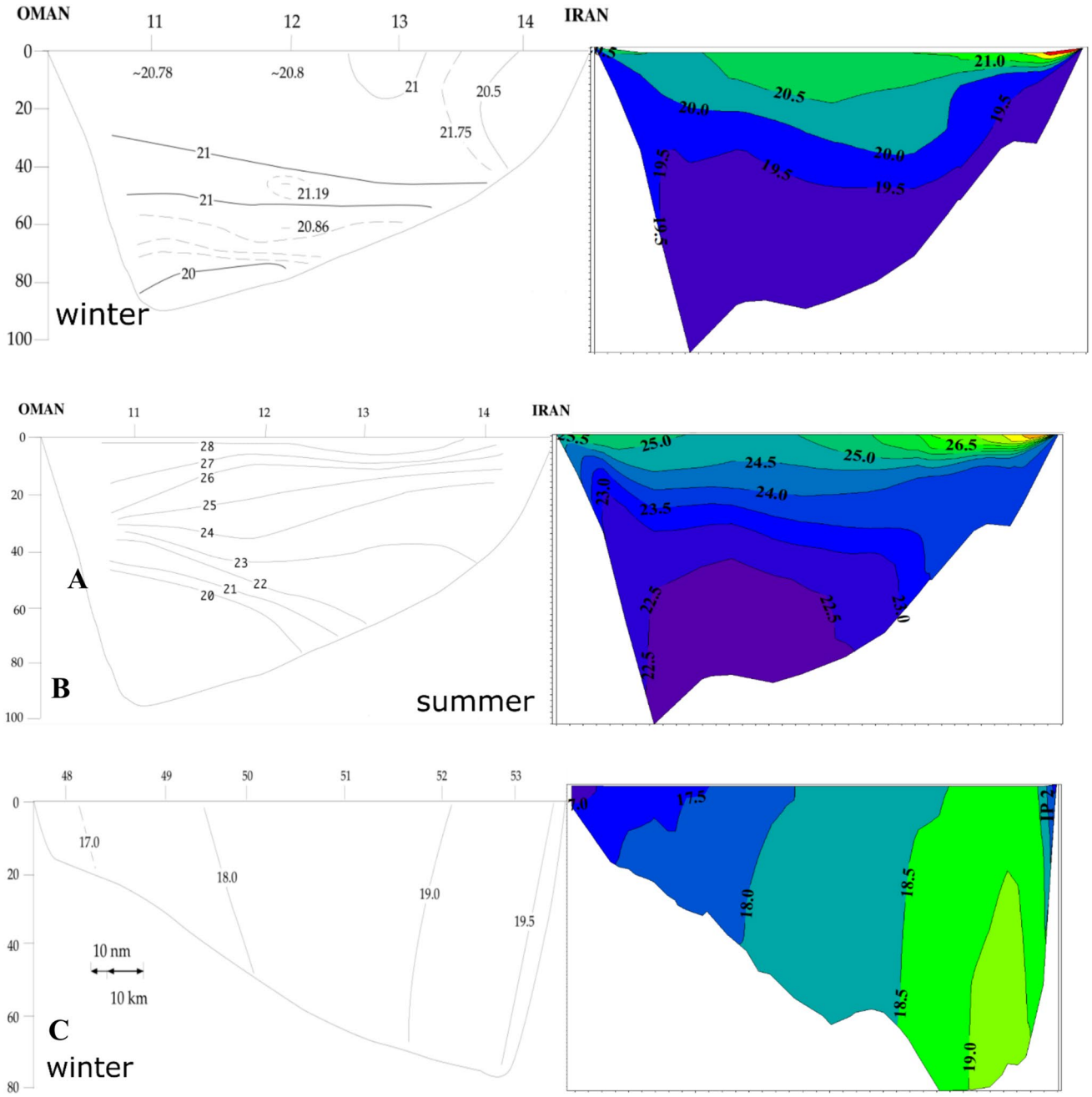

Fig. 13 The vertical temperature profile Measured (left) versus simulated (right), **a**: section C in winter; **b**: section C in summer; **c**: section I in winter; **d**: section I in summer

0.1 psu. This is compatible with the previous findings such as the one reported by (Chow et al. 2019). He stated that desalination does not have a large long-term effect on average water salinity due to the soothing effect of the Indian Ocean. However, it should be noted that the contour values in Fig. 21 show the average annual values, while the maximum instant values are clearly more than the averaged ones. For instance, (Lee and Kaihatu 2018), employing Delft3D-FLOW software, reported that the maximum increase in water salinity of the PG due to the presence of desalination plants occurs at JabalAli in UAE with the value of 4.21 ppt during the fall season. They reported the maximum salinity increases at six major stations in the PG located in UAE, Saudi Arabia, Qatar, Bahrain, Kuwait, and Iran, in the order of the highest to the lowest increase in salinity. The minimum value was 0.43 ppt at Asaluy in the northern part of the PG at the coast of Iran. However, an average value is generally more reliable since its numerical error is usually

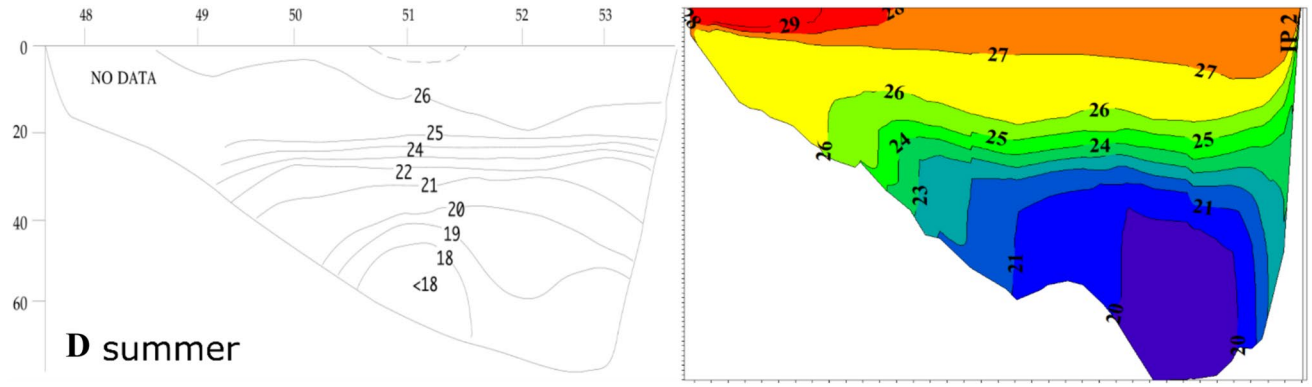

Fig. 13 (continued)

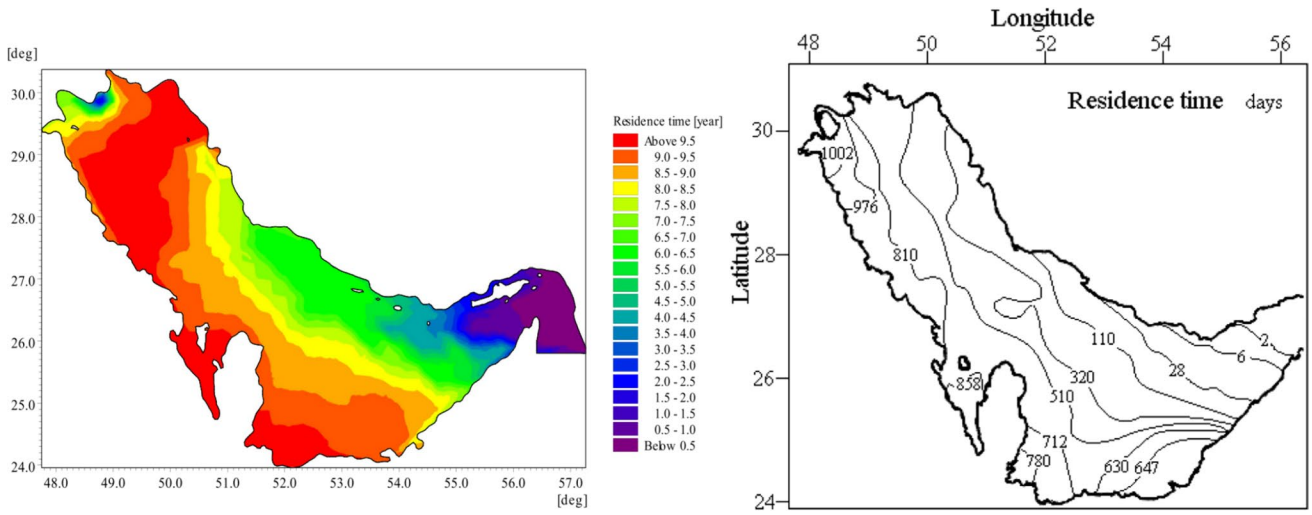

Fig. 14 Water residence time based on the previous studies; left side: Alosairi et al. (2011) and right side: Ranjbar et al. (2020)

less than the value of a local maximum point. In addition, it is an important parameter for making general decisions considering the long-term effects. Therefore, following the concern of this study, the averaged values are investigated and discussed in more detail in the following.

To further investigate the excess salinity in PG, the averaged salinity increases for the two line sections C and I are depicted in Fig. 22. The former section is located near the Strait of Hormuz and the latter one at the center of the PG (as shown in Fig. 10).

Following the water circulation in the PG, fresh and low-salinity water enters the PG from the surface layers at section C and the salty water exits from the deep depths. This area is also located far from big desalination plants with high effluents, allowing the effluents sufficient time to disperse in the water. As a result, increasing the desalination brines does not have a significant effect on the salinity pattern in this section. As depicted in Fig. 21 (diagrams a, c, and e), a relatively uniform increase in water salinity with the same pattern as water circulation occurs in this section. However, as anticipated, doubling the wastewaters has relatively more impact than the 50% brine increases. On the other hand, as shown in Fig. 22 (diagrams b, d, and f), the southern shallow regions of section I experience the most salinity increase, while only a slight salinity increase occurs along the northern coasts. The deep points of this section are also more sensitive to the excess salinities. However, compared to the scenario without desalination facilities in the PG, a 100% increase in wastewater discharge resulted in a maximum increase of 0.15 psu in water salinity. However, diagrams a, c, and e depict an increase in water salinity at section C along both the southern and northern shores. This phenomenon is also observable in Fig. 21.

The effect of creating new facilities on the northern shores of PG

For any new water desalination plant, it is essential to determine a proper outfall location. As discussed in the previous

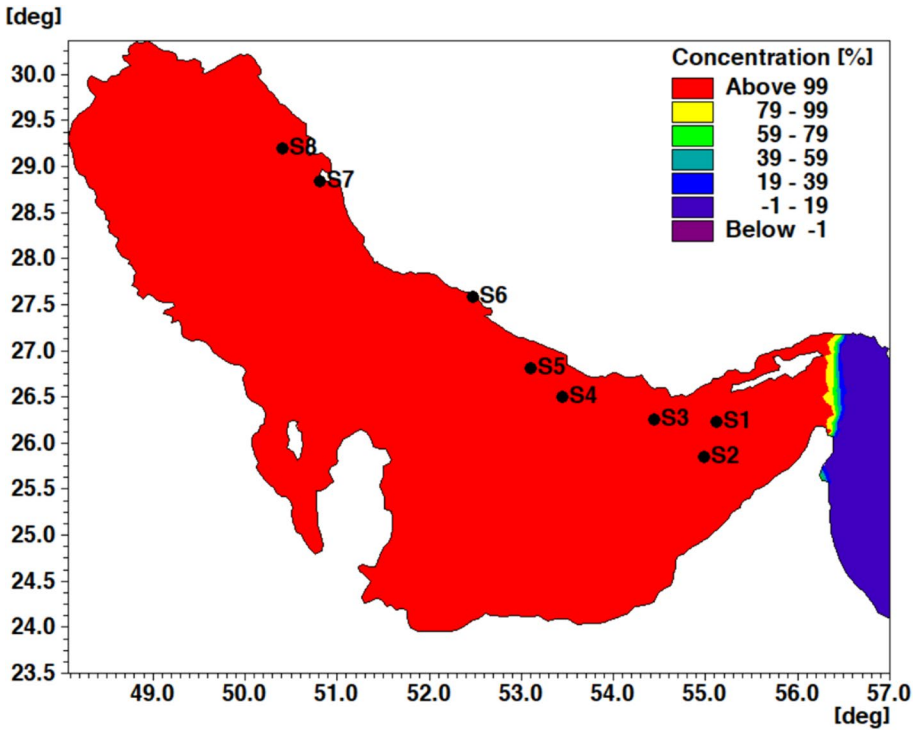

Fig. 15 Initial concentration defined in transport module

section, the mean salinity of PG does not change noticeably by developing the current desalination plants. In addition, due to probable water scarcity in future years, a solution ahead the countries is developing new big desalination plants near the shorelines to provide the required desalinated water. It is clear that the location of desalination plants not only depends on environmental criteria but also the distance to the target consumption point. The limitations and coastline lengths in each country are other factors too. Five Arab countries exist along the southern coastlines of the PG, while the longest coastline belonging to Iran on the northern side. Therefore, it is important to find the best location for new desalination plants along the northern shorelines. In addition, as shown in previous sections (see Figs. 9, 12, 22), pollutants from the northern regions will flow toward the southern parts due to natural current patterns and subsequently remain a long time in the PG. Therefore, to investigate the impact of new desalination plants on the salinity of PG, the northern coastlines have been divided into four zones as depicted in Fig. 23. Each zone is investigated by adding two wastewater points. The current situation, including only existing desalinations, is considered as a baseline or normal condition, and four simulations have been conducted to examine the impact of building new water desalination plants. Each simulation involved the addition of two large desalination plants with a daily capacity of 500 thousand cubic meters in a zone. For instance, sources S1 and S2 are activated in the first simulation, S3 and S4 in the second, S5 and S6 in the third, and S7 and S8 in the fourth simulation. Afterward, the results are compared with the normal state to examine the impact of constructing new facilities in each of these four regions. In addition, RO system is assumed for all the new desalination plants since it has been a common system in recent years. Based on these assumptions, the salinity of each outfall source is considered to be 20 psu more than the ambient conditions around that source.

The salinity over the PG's surface area is averaged, and the time series of the mean values are depicted in Fig. 24 for all the considered scenarios, in comparison with the normal (existing) condition. As shown in this figure, the establishment of additional water desalination plants in the northern regions does not indicate any impact and a substantial increase in the mean salinity levels of the PG.

To investigate the different regions of the PG more precisely, the average increase in water salinity due to the creating of new desalination plants is depicted in Fig. 25. Again, these data do not indicate any significant increase in the average salinity level, and therefore, it can be concluded that the impact of new sources is generally negligible. The only exception is the fourth region, where sources S7 and S8 are near Qeshm Island. As shown in Fig. 21, the area above this Island is special and susceptible to developing new desalination facilities. As discussed in the previous section, there exist some brine effluents in this area on the one hand and the current speed is high in this region on the other hand. To further investigate the situation of this region, Fig. 26 presents the vertical profile of the residual current at two sections around Qeshm

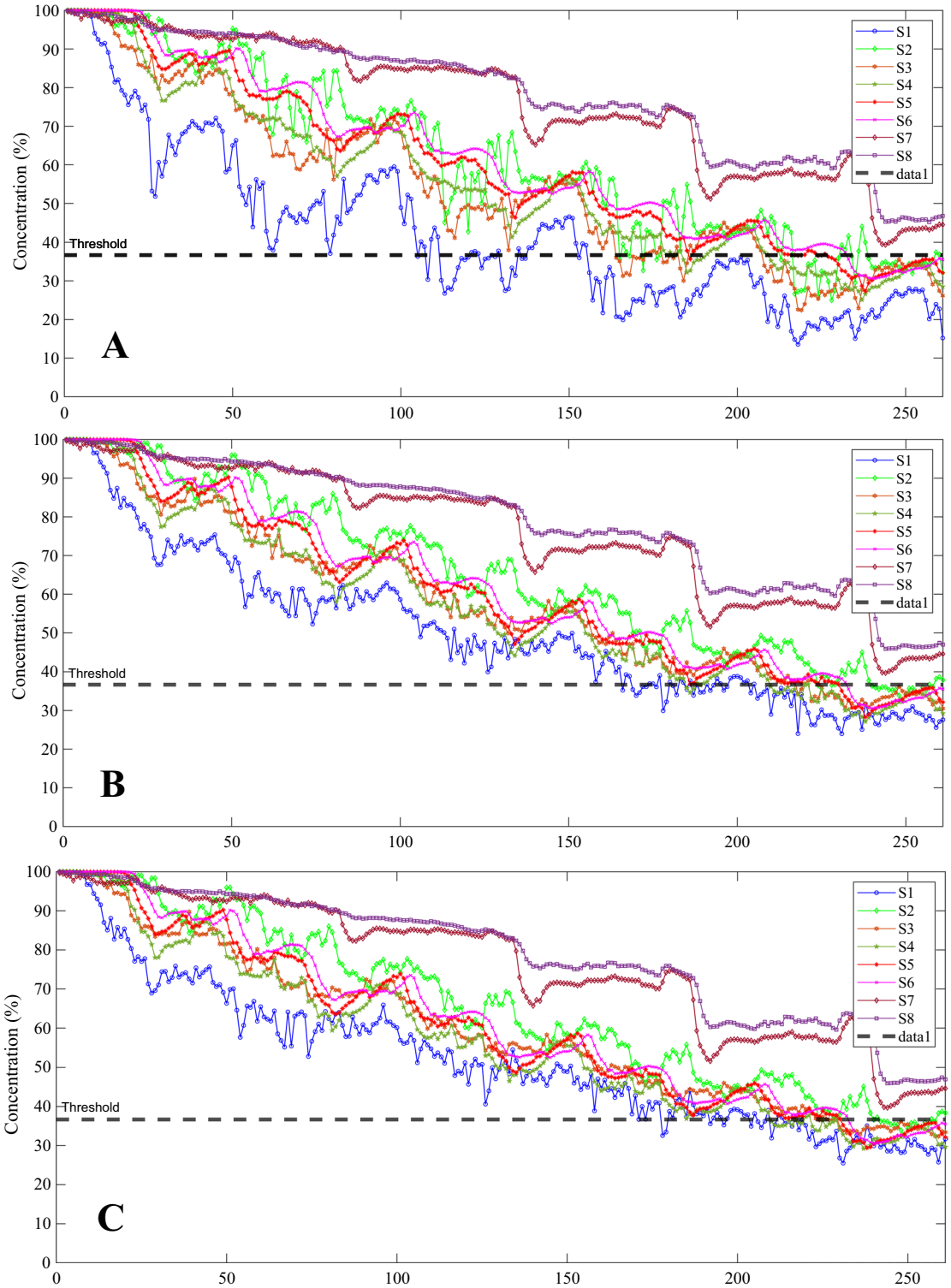

Fig. 16 The reduction of pollutant concentration at each of the points shown in Fig. 14 versus the number of the weeks, **a**: in the surface layer; **b**: in the middle layer; and **c**: in the bottom layer

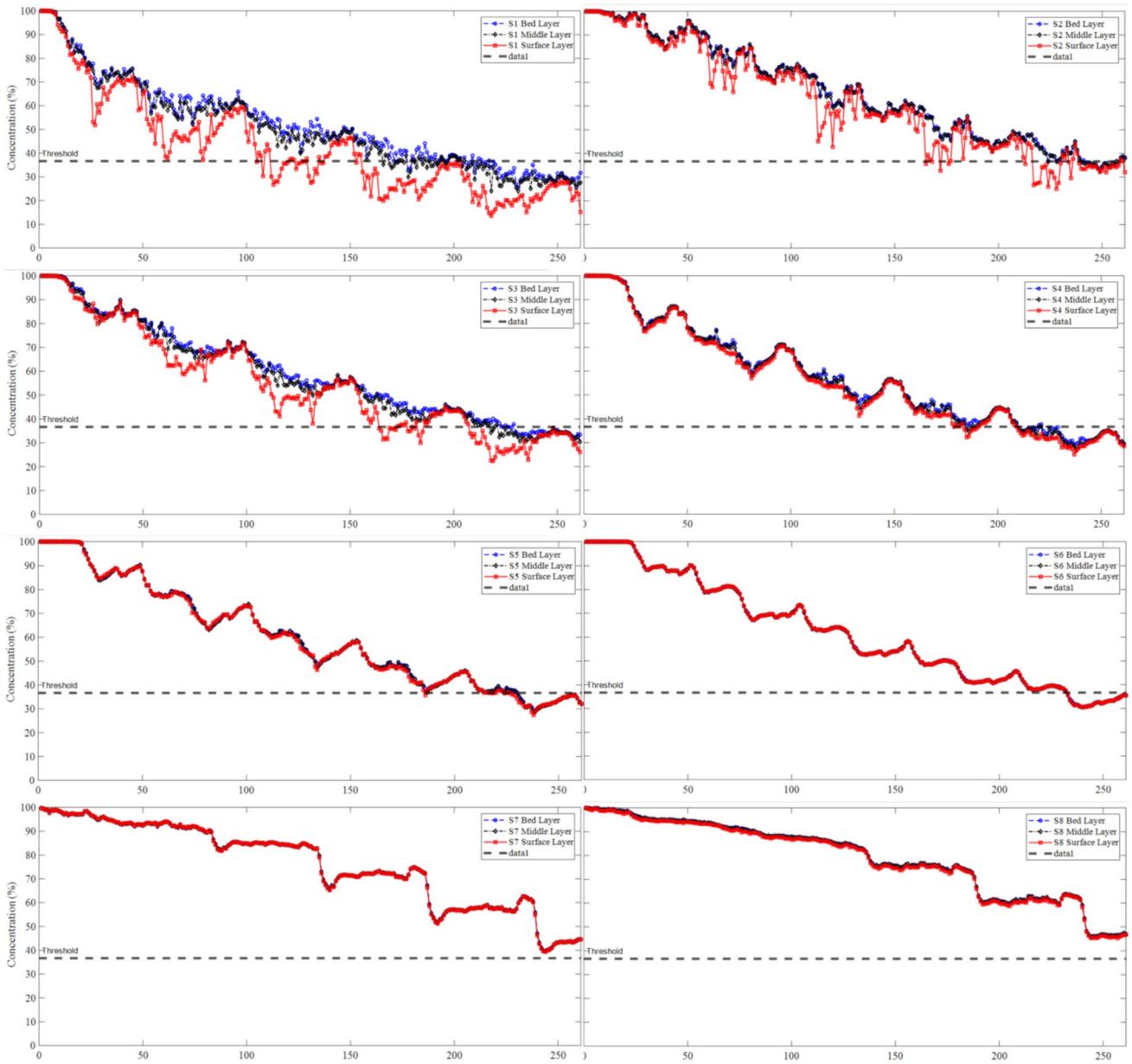

Fig. 17 Pollutant concentration versus the number of weeks at different depths for the points in Fig. 15

Island. As shown in this figure, the north of Qeshm Island is a shallow region with an average depth of nearly 5 m. Therefore, the volume of seawater is insufficient to effectively dissipate the pollutants. Furthermore, the direction of residual currents is eastward in this region, generating a continuous eastward flow that transports the pollutions from sources S7 and S8 to this region. These factors result in the accumulation of pollutants above Qeshm Island. Although these two sources increase the mean water salinity locally, the increase in the mean salinity of PG is still negligible, as depicted in Fig. 24.

Table 5 displays the proportion of water exchanges in the PG from various sources. According to this table, the majority of the freshwater that enters the PG through the Strait of Hormuz will be compensated with evaporation, while the volume of brine discharge is one order less than the other sources. Therefore, in comparison with desalination brines, evaporation has a much greater impact on controlling the

Table 4 Point coordinates and water residence time at each point in the vertical layers

point ID	Longitude (Degree)	Latitude (Degree)	water residence time at Surface layer (month)	water residence time at Middle layer (month)	water residence time at Bottom layer (month)
S1	55.1150	26.2339	26	43	45
S2	54.9794	25.8500	42	55	58
S3	54.4434	26.2550	40	55	59
S4	53.4402	26.5060	45	48	48
S5	53.1037	26.8103	48	48	48
S6	52.4764	27.5837	59	59	59
S7	50.8093	28.8404	65 <	65 <	65 <
S8	50.4120	29.1907	65 <	65 <	65 <

salinity of water, and it can even control the net volume of water exchange through the Strait of Hormuz.

Based on the presented results, it can be generally concluded that creating new desalination plants along the northern coasts of the PG does not contribute to increasing the mean salinity of the PG. These results are compatible with previous findings, such as the one presented by (Ibrahim et al. 2020), which concluded that by increasing the capacity of desalination facilities, the average salinity across the PG does not increase. His results also showed that the current salinity balance of the PG is stable and is not likely to change under atmospheric and ocean climate conditions. It should be noted that the conclusions in this study are restricted to the assumed effluent discharges. As shown in Sect. "Results and discussion"–"Materials and methods," doubling the discharge of all the existing discharges has an effect (yet negligible) on the mean salinity of the PG. On the other hand, the impact of rainfall and evaporation rate, river inlet discharges, water climate changes, and discharge of water exchanges between the PG and Oman Sea seem to be more important factors in the mean salinity of the PG than the effect of the desalination effluents. This can be concluded based on comparing the amount of brine discharges with the other parameters as reported in Table 5.

In the end, it should be emphasized that although salinity increases due to the development of desalination plants are not considerable, and literature reviews indicate that physiological impacts are rarely occurring below salinity increases of 2–3 ppt, it is suggested to consider the development of desalination plants more comprehensively by taking into account other mitigation options such as improvement of recovery efficiency of desalination plants in the future with smaller volumes of pollutions or using zero brine technologies or appropriate positioning of intakes/outfalls in conjunction with other affecting factors those may compromise the sustainable development of PG such as global climate change, sea-level rise due to global warming on the one hand and more evaporation on the other hand, reduction of river supply and change of precipitation patterns, human impacts, and socio-economical and water demands of the adjacent countries. Clearly, investigating all of these factors is beyond the scope of one study. Still, it seems that performing different studies is essential to obtain more comprehensive results about the future environment of the PG.

Conclusion

This study investigates the salinity of PG by taking into account the brine discharges from existing desalination plants as well as future ones. For this regard, a validated numerical model is utilized and the current pattern and water circulation inside PG are determined. The water residence time is also calculated for different locations, and the potential impact of new desalination plants on the salinity of PG is studied afterward. The novel contributions of this work include the integration of climate change scenarios and a detailed assessment of regional salinity variations.

The results of this study indicate that the water residence time (required time to reach 37% of the initial pollution) in the PG varied across different regions and depths, taking between 26 and 65 months from the areas near the Strait of Hormuz to the northwestern and southern regions of the

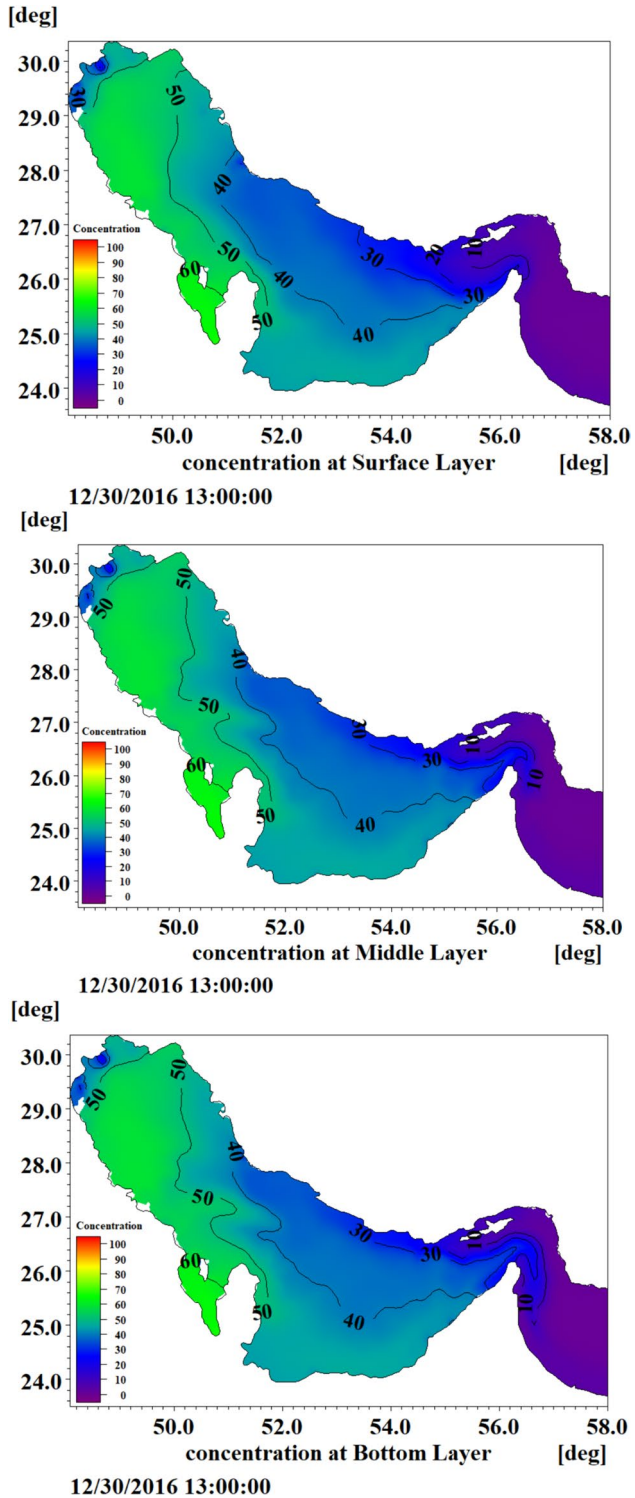

Fig. 18 The pollutant concentration in different vertical layers of the PG after 5 years

PG. In addition, freshwater enters the PG from the northern shallower sections of the Strait of Hormuz and salty water moves out from the deep layers. The input water flows generally along the north coasts of PG, and some part of this flow turns toward the south when it reaches the middle of the PG. Another part of the flow goes forward and then inclines to the southern regions. Therefore, the counterclockwise flow in the PG mitigates the impact of effluent discharge from the northern coast and redirects it toward the south regions. It is demonstrated that the southern areas of PG are more sensitive to salinity increase than the north areas. The salinity level is more in the south regions where most desalination plants are also working.

On the other hand, the total volume of brine water released into the PG from desalination plants is nearly only 0.2% of the water that goes out of the PG through the Strait of Hormuz. In addition, it is only 2.68% of the water loss from the PG due to evaporation. As such, any increase in desalination capacity would have a negligible impact on the salinity of the PG when compared to the effects of water evaporation. Although the impact of desalination plants on the mean salinity of the PG is negligible (nearly 0.01 psu), the local effects are more detectable in some areas as discussed in Sect. "Results and discussion"–"Materials and methods." However, these effects are not considerable yet in comparison with the evaporation effect. For example, doubling the capacity of existing desalination plants has the most effect on the local salinity but is limited to nearly 0.2 psu at the southern regions of the PG as well as at the northern parts of the Qeshm Island as depicted in Fig. 21. In addition, construction of two new big desalination plants (each with a capacity of 500,000 m^3/day) in the northern parts of the Qeshm Island has a more noticeable effect on the salinity levels than locating these brines at other northern coasts of the PG.

The results of this study provide valuable information for understanding the salinity pattern, residence time, pollutant concentration in the PG, and its sensitivity to brine waters from desalination plants. It also shows the importance of locating new desalination facilities properly within the PG to minimize local environmental impacts, and it can be used to develop effective strategies for managing and mitigating pollution in this region. In addition, this research provides a comprehensive assessment of the long-term impacts of desalination plants on the PG's salinity. Based on a calibrated 3D model and after modeling different desalination development scenarios, it is concluded that the overall increase in the mean salinity of the PG is minimal. However, there are some local areas sensitive to the salinity effects significantly. The study highlights the necessity of investigating the global effect of any new desalination plant on the accumulated excess salinity in other areas. Doing such a regional study can improve the sustainability of water management practices in the PG. Some suggestions for future works are enhancing numerical models to include more variables and considering more scenarios including

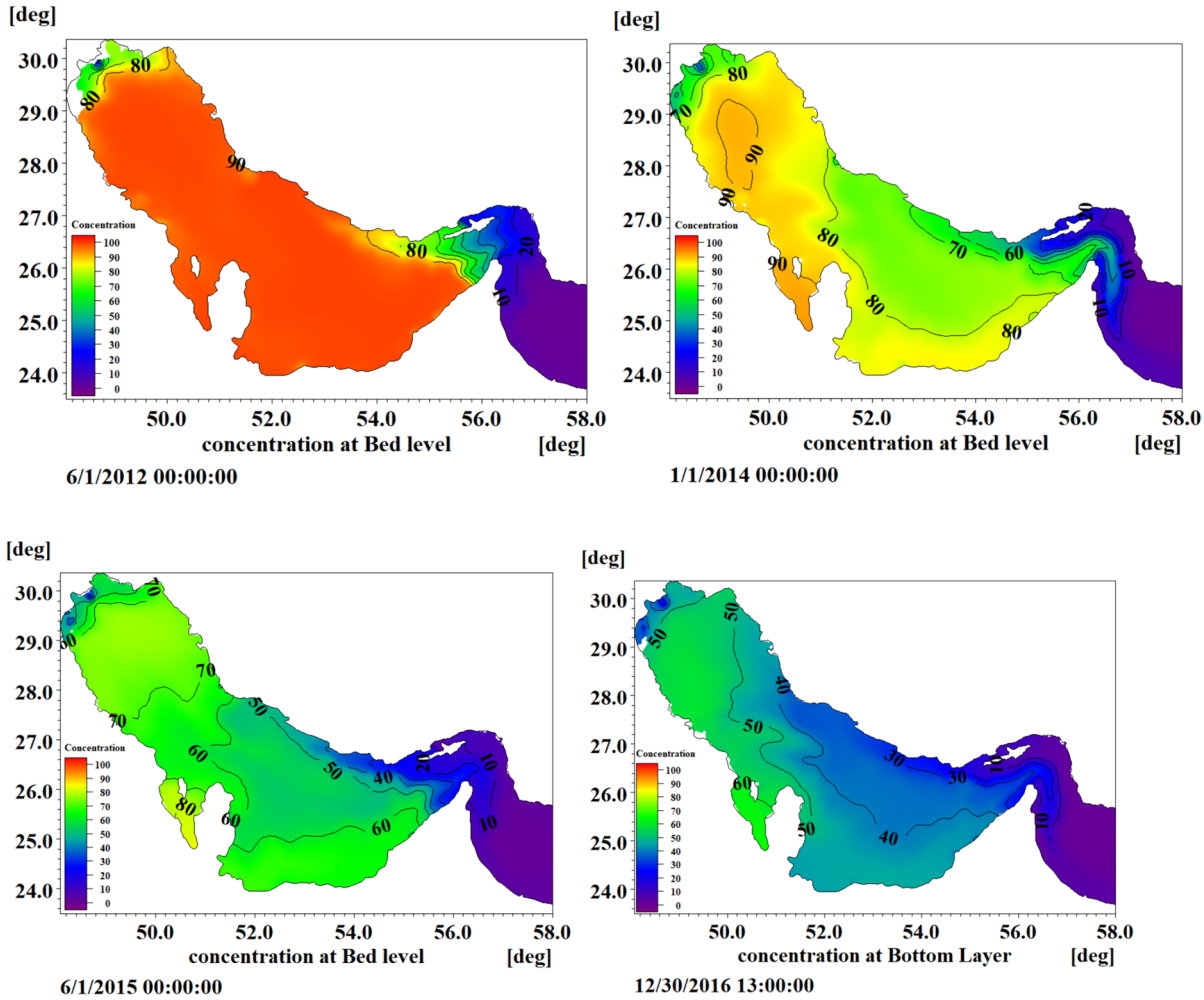

Fig. 19 Change of pollutant concentration at the bed layer over time

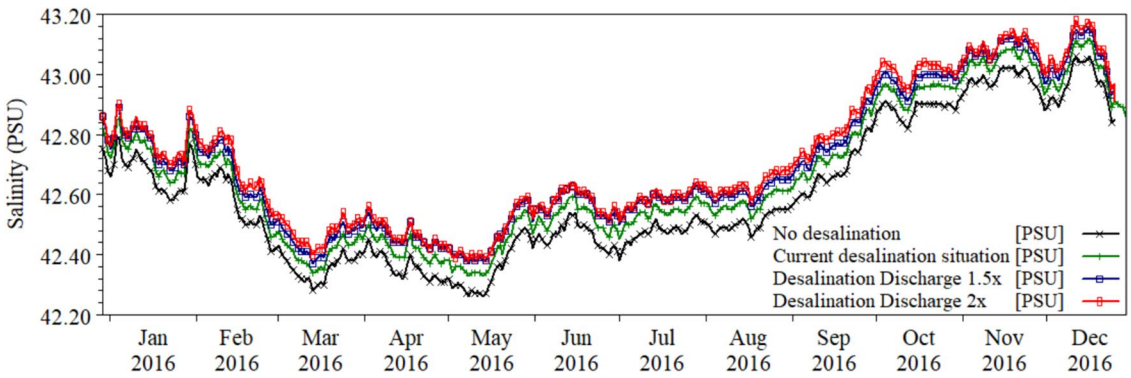

Fig. 20 Changes in the average salinity of surface water in the PG due to increasing the discharges from desalination plants

climate changes. In addition, providing an international plan to resolve the scarcity of desalinated water in the neighboring countries with minimal general effects on semi-enclosed PG can be so useful. Possibility of using renewable energies to reduce environmental impacts can be also an alternative besides new desalination processes and wastewater treatment technologies.

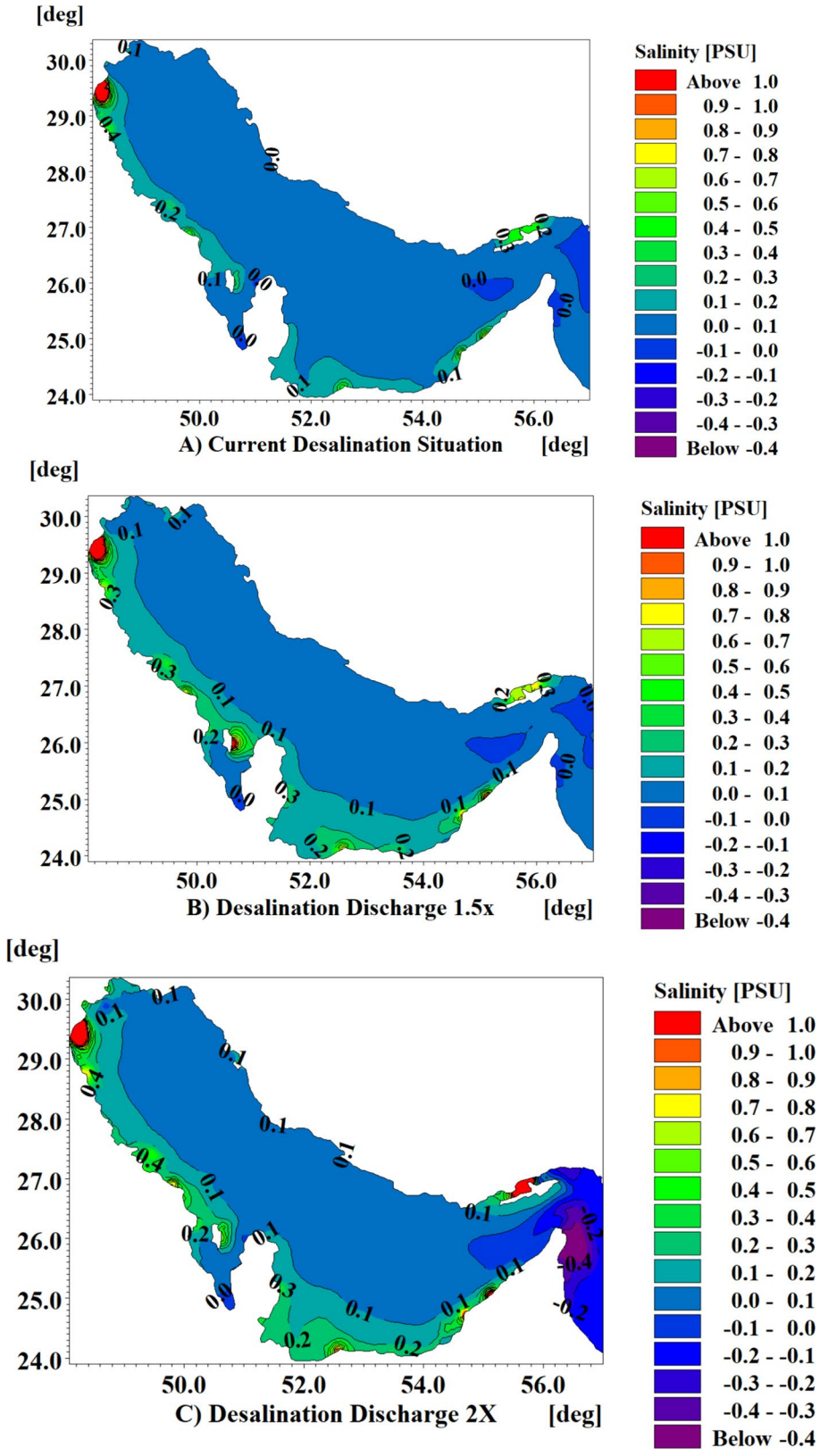

Fig. 21 The average increase in salinity compared to the state without any desalination plants, a: existing desalinations, b: 50% increase in discharges, c: 100% increase in discharges

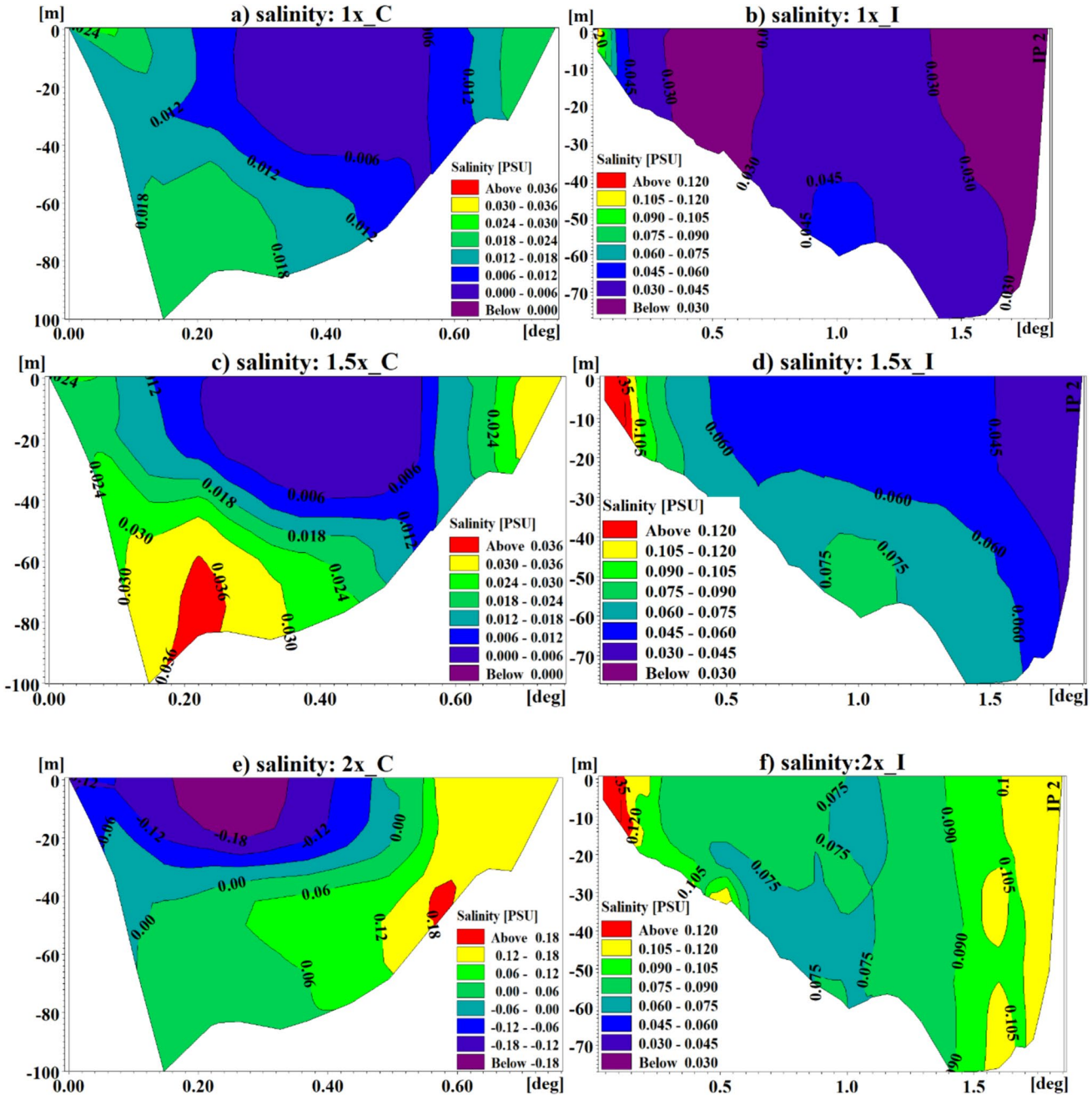

Fig. 22 The vertical profile of the average salinity increases in sections C (left) and I (right) due to the increase in the effluent flows compared to the condition without any desalination facilities

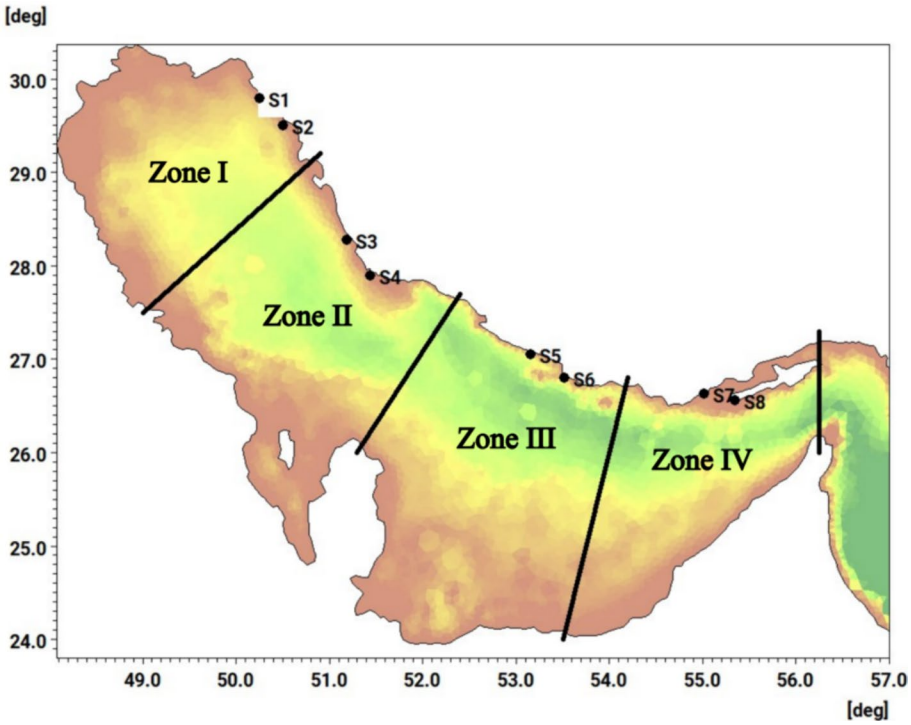

Fig. 23 Illustration of new brine sources along the northern coast of the PG

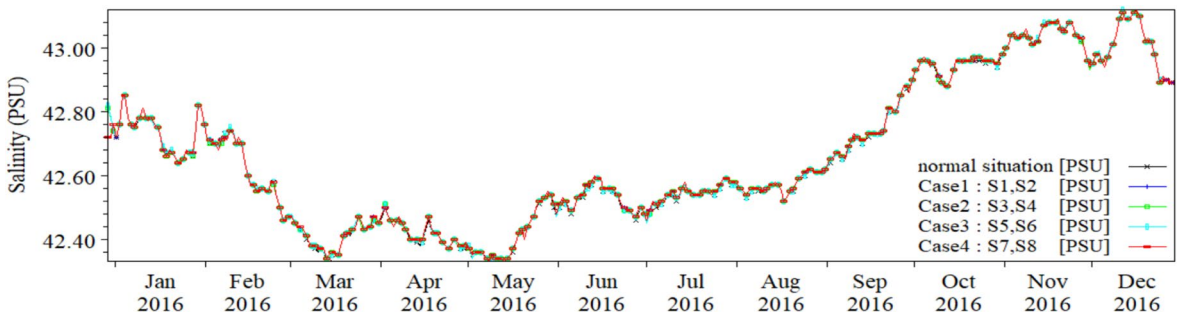

Fig. 24 Comparison of the average salinity of the PG according to creating new facilities

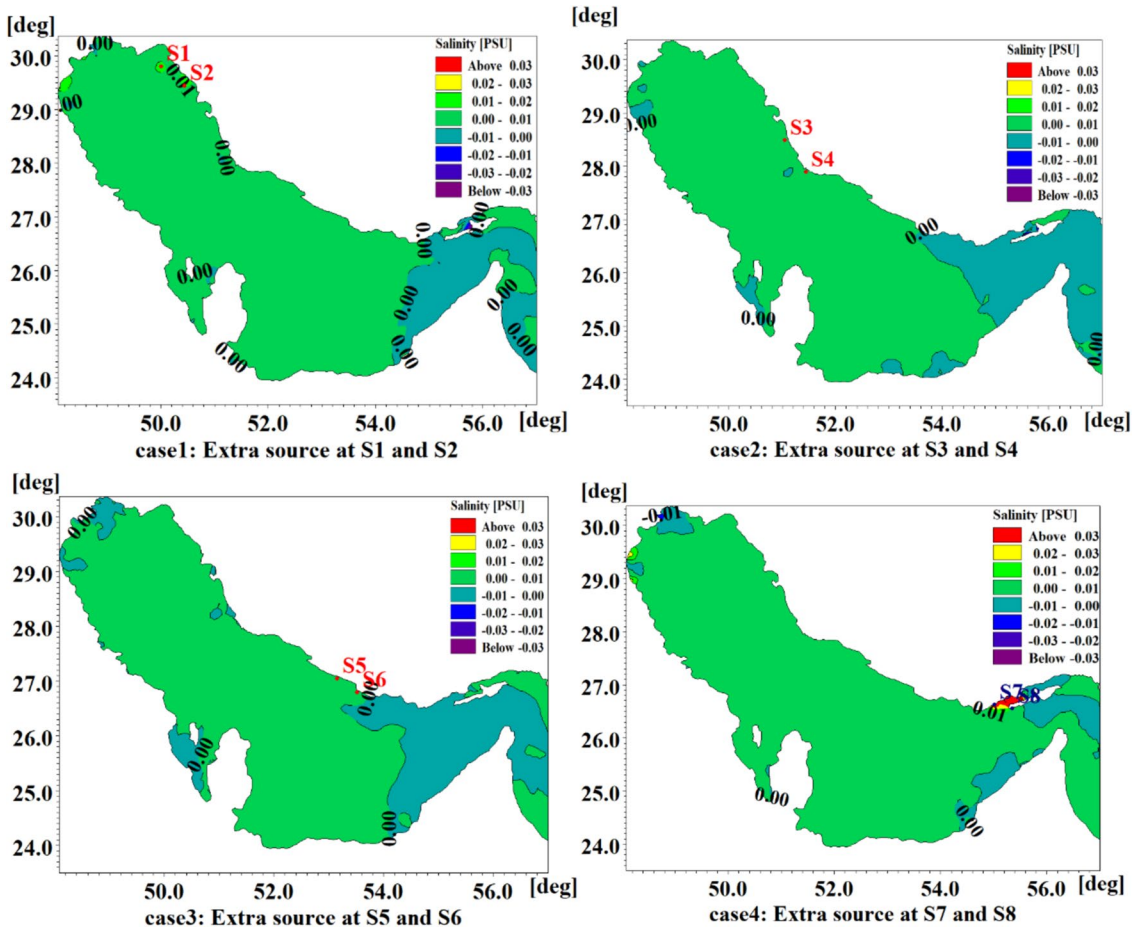

Fig. 25 Mean increase in PG surface water salinity due to the addition of extra sources; **a**: sources S1 and S2; **b**: sources S3 and S4; **c**: sources S5 and S6; and **d**: sources S7 and S8

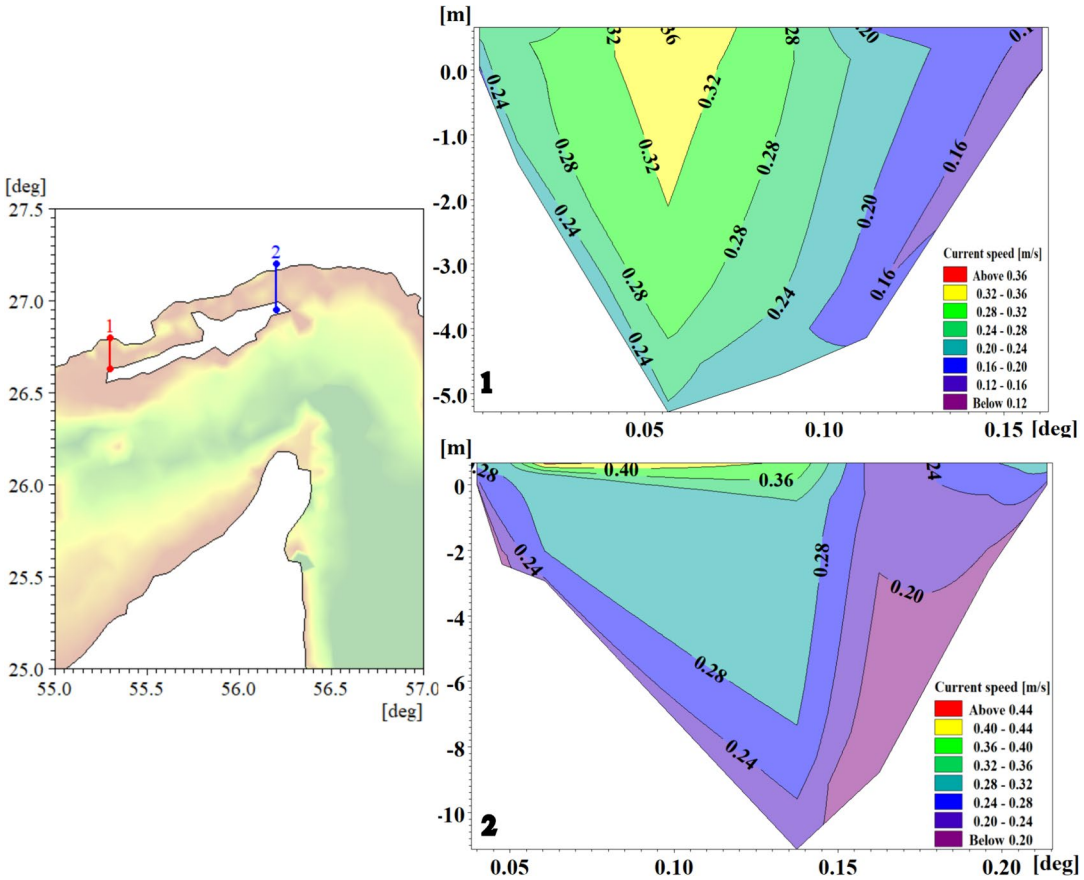

Fig. 26 Vertical profile of the residual current in the north of Qeshm Island

Table 5 A summary of the amount of water entering the PG from different sources

Sources	Discharge (Billion m^3/year)	The normalized value to the discharge of existing desalination plants
Incoming water from the Oman Sea	7198.68	588.18
Outgoing water to the Oman Sea	6787.60	554.59
Net exchanged water through the Strait of Hormuz	411.08	33.59
Net water loss in the Persian Gulf (Evaporation minus rainfall and rivers)	384.79	31.44
Brine discharge from existing desalination plants	12.24	1.00

Appendix A: Table of notations

Notation	Definition	Notation	Definition
x, y, z	Cartesian coordinate components	u, v, w	Orthogonal components of velocity along x, y, and z directions
t	Time	$h=d+\eta$	Total water depth
$f=2\Omega\sin(\varphi)$	Coriolis parameter	η	water elevation
Ω	Angular speed of the Earth's rotation	d	still water depth
φ	latitude	g	gravity acceleration
ρ	water density	Sxx, Sxy, Syx, Syy	Radiation stress tensor components
vt	Vertical eddy viscosity	pa	atmospheric pressure
0ρ	Initial density of water	S	Discharge amount at the source point
us, vs	The speed of water discharge into the water environment in the x and y directions	Fu, Fv	Horizontal stress in x and y directions
A	Horizontal eddy viscosity	$\hat{P}, \hat{E}$	Precipitation and evaporation rates
τ_{bx}, τ_{bx}	Components of water surface tension with the seabed in x and y directions	τ_{sx}, τ_{sx}	Components of water surface tension with wind along x and y directions
$\overline{u}, \overline{v}$	Depth-averaged velocities	D_v	Turbulence diffusion coefficient in the vertical direction
F_T, F_s	Term of horizontal spread of temperature and salinity	$\hat{H}$	source of heat exchange with the atmosphere
D_h	Horizontal spread coefficient	Q_n	Net heat flux on the water surface
c_p	Specific heat of water 4217 = J/(kg°K)	q_v	Latent heat flux
l_v	Latent heat of vaporization of water = 2.5×106	v_t	Eddy viscosity
k	Kinetic energy of turbulence per unit mass	ε	Turbulence Kinetic Energy Dissipation
P	shear coefficient	B	Buoyancy coefficient
β	Fraction of light energy absorbed near water surface	λ	Light attenuation coefficient
L	heat of vaporization = 2.5.106 J/kg	C_e	Moisture transfer coefficient = 1.32.10–3
W_{2m}	Wind speed at a height of 2 m above the water surface	Q_{water}	Evaporation density of water
Q_{air}	Evaporation density of water in the atmosphere		

Funding The author(s) received no specific funding for this work.

Declarations

Conflict of interest On behalf of all authors, the corresponding author states that there is no conflict of interest.

Ethical approval This essay does not have any ethical problems, and international standards regarding human and animal rights have been observed.

References

Afshar-kaveh N et al. (2016) Evaluation of different wind fields for storm surge modeling in the Persian Gulf. J Coast Res 33(3):596. https://doi.org/10.2112/jcoastres-d-15-00202.1

Akbari H, Ebrahimi MH (2016) Near field mixing of multi-diffuser dense jets in shallow water condition and ambient currents. In: 15th Iranian hydraulics conference. Available at: https://civilica.com/doc/562894

Al-Mutaz IS (1991) Operation of dual purpose MSF plants at water/power peak demand. Desalination 84(1–3):105. https://doi.org/10.1016/0011-9164(91)85121-A.

Alosairi Y, Imberger J, Falconer RA (2011) Mixing and flushing in the Persian Gulf (Arabian Gulf). J Geophys Res Oceans 116(3):1–14. https://doi.org/10.1029/2010JC006769.

Campos EJD et al (2020) Freshwater budget in the Persian (Arabian) Gulf and exchanges at the Strait of Hormuz. PLoS ONE. https://doi.org/10.1371/journal.pone.0233090

Chow AC et al. (2019) Numerical prediction of background buildup of salinity due to desalination brine discharges into the northern Arabian Gulf. Water (Switzerland), 11(11):1–14. https://doi.org/10.3390/w11112284

Dhi (2013) MIKE 21 & MIKE 3 flow model fm hydrodynamic module, p 14

Elhakeem A, Elshorbagy W (2013) Evaluation of the long-term variability of seawater salinity and temperature in response to natural and anthropogenic stressors in the Arabian Gulf. Mar Pollut Bull 76(1–2):355–359. https://doi.org/10.1016/j.marpolbul.2013.08.036

Elhakeem A, Elshorbagy W (2015) Hydrodynamic evaluation of long term impacts of climate change and coastal effluents in the Arabian Gulf. Mar Pollut Bull 101(2):667–685. https://doi.org/10.1016/j.marpolbul.2015.10.032

Elhakeem A, Elshorbagy W, Bleninger T (2015) Long-term hydrodynamic modeling of the Arabian Gulf. Mar Pollut Bull 94(1–2):19–36. https://doi.org/10.1016/j.marpolbul.2015.03.020.

Gray S et al. (2011) Seawater use and desalination technology. Treatise Water Sci, pp. 73–109. https://doi.org/10.1016/B978-0-444-53199-5.00077-4

GEBCO (2022) Available at: https://doi.org/10.5285/e0f0bb80-ab44-2739-e053-6c86abc0289c.

Höpner T, Windelberg J (1997) Elements of environmental impact studies on coastal desalination plants. Desalination, 108(1–3):11–18. https://doi.org/10.1016/S0011-9164(97)00003-9

Hosseinibalam F, Hassanzadeh S, Rezaei-Latifi A (2011) Three-dimensional numerical modeling of thermohaline and wind-driven circulations in the Persian Gulf. Appl Math Model 35(12):5884–5902. https://doi.org/10.1016/j.apm.2011.05.040

Hunter JR (1983) Circulation of the Arabian Gulf, pp 31–42

Ibrahim HD et al (2020) Multiple salinity equilibria and resilience of Persian/Arabian Gulf Basin salinity to brine discharge. Available at: https://doi.org/10.3389/fmars.2020.00573

Iqbal M (1983) An introduction to solar radiation. Elsevier Inc., British Columbia. https://doi.org/10.1016/B978-0-12-373750-2.X5001-0

Kämpf J, Sadrinasab M (2006) The circulation of the Persian Gulf: a numerical study. Ocean Sci 2(1):27–41. Available at: https://doi.org/10.5194/os-2-27-2006

Kamranzad B (2018) Persian Gulf zone classification based on the wind and wave climate variability. Ocean Eng 169:604–635. https://doi.org/10.1016/j.oceaneng.2018.09.020

Khan NY, Al-ajmi D (1998) Post-war imperatives for the sustainable 24(l):239–248. https://doi.org/10.1016/S0160-4120(97)00141-4

Lee W, Kaihatu JM (2018) Effects of desalination on hydrodynamic process in Persian Gulf. Coastal Eng Proc 36:3. https://doi.org/10.9753/icce.v36.papers.3

Li D, Anis A, Al Senafi F (2020) Physical response of the Northern Arabian Gulf to winter Shamals. J Mar Syst. https://doi.org/10.1016/j.jmarsys.2019.103280

Mahpeykar O, Khalilabadi M (2021) Numerical modelling the effect of wind on water level and evaporation rate in the Persian Gulf, 5(1)

Michael Reynolds, R. (1993) Physical oceanography of the Gulf, Strait of Hormuz, and the Gulf of Oman-Results from the Mt Mitchell expedition. Mar Pollut Bull 27(C):35–59. https://doi.org/10.1016/0025-326X(93)90007-7

Munk WH, Anderson ER (1948) Notes on a theory of the thermocline. J Mar Res 7(3)

Oddo P, Pinardi N (2008) Lateral open boundary conditions for nested limited area models: a scale selective approach. Ocean Modell 20(2):134–156. https://doi.org/10.1016/j.ocemod.2007.08.001.

Paparella F, D'Agostino D, Burt JA (2022) Long-term, basin-scale salinity impacts from desalination in the Arabian/Persian Gulf. Sci Rep 12(1):1–12. https://doi.org/10.1038/s41598-022-25167-5

Pous S, Lazure P, Carton X (2015) A model of the general circulation in the Persian Gulf and in the Strait of Hormuz: intraseasonal to interannual variability. Continental Shelf Res 94:55–70. https://doi.org/10.1016/j.csr.2014.12.008

Pous SP, Carton X, Lazure P (2004) Hydrology and circulation in the Strait of Hormuz and the Gulf of Oman-Results from the GOGP99 Experiment: 1. Strait of Hormuz. J Geophys Res Oceans 109(12):1–15. https://doi.org/10.1029/2003JC002145

Rahmani Firozjaei M et al (2023) Evaluation of seawater intake discharge coefficient using laboratory experiments and machine learning techniques Evaluation of seawater intake discharge coefficient using laboratory experiments and machine learning techniques. Ships Offshore Struct. https://doi.org/10.1080/17445302.2023.2247125

Ranjbar MH, Etemad-Shahidi A, Kamranzad B (2020) Modeling the combined impact of climate change and sea-level rise on general circulation and residence time in a semi-enclosed sea. Sci Total Environ 740:140073. https://doi.org/10.1016/j.scitotenv.2020.140073.

Rodi W (2017) Turbulence models and their application in hydraulics: a state-of-the-art review, third edition. Available at: https://doi.org/10.1201/9780203734896

Sadrinasab M, Kämpf J (2004) Three-dimensional flushing times of the Persian Gulf. Geophys Res Lett 31(24):1–4. https://doi.org/10.1029/2004GL020425

Sheppard C et al. (2010) The Gulf: a young sea in decline. Mar Pollut Bull 60(1):13–38. https://doi.org/10.1016/j.marpolbul.2009.10.017

Smagorinsky J (1963) General Circulation Experiments With The Primitive Equations: I. The Basic Experiment. Monthly Weather Rev 91(3):99–164. https://doi.org/10.1175/1520-0493(1963)091<0099:GCEWTP>2.3.CO;2.

Swift SA, Bower AS (2003) Formation and circulation of dense water in the Persian/Arabian Gulf. J Geophys Res Oceans 108(1):1–22. https://doi.org/10.1029/2002jc001360

Thomann RV, JAM (1987) Principles of surface water quality modeling and control, Harper-Collins

UNESCO (1981) The practical salinity scale 1978 and the international equation of state of seawater. UNESCO technical papers in marine science, p 36

Wu J (1980) Wind-stress coefficients over sea surface near neutral conditions—a revisit. J Phys Oceanogr 10(5):727–740. https://doi.org/10.1175/1520-0485(1980)010<0727:WSCOSS>2.0.CO;2

Xue P, Eltahir EAB (2015) Estimation of the heat and water budgets of the Persian (Arabian) gulf using a regional climate model. J Clim 28(13):5041–5062. https://doi.org/10.1175/JCLI-D-14-00189.1

Yao F (2008) Water mass formation and circulation in the Persian Gulf, and Water exchange with the Indian Ocean the hydrogaphy and circula-, University of Miami